DEVELOPMENT OF AN ARTICULATING ROBOTIC ARM FOR SPRAY PAINTING ON ROADWAYS

Robert Henry Olshausen

AHMCT Research Report

UCD-ARR-98-01-15-01

Final Report of Contract

RTA 65X936

January 15, 1998

University of California at Davis
California Department of Transportation

THE
BIG
ARTICULATED
STENCILING ROBOT
(BASR)*

Volume II

Phillip W. Wong, P.E.
Professor Bahram Ravani
Richard Blank
Jeff Hemenway
Richard McGrew
Ulrich Mueller
Dr. Walter Nederbragt
Robert Olshausen
Ken Sprott

January 15, 1998

DISCLOSURE STATEMENT

Design information, processes and techniques discussed within this report may be patent pending. Do not disclose to other agencies, persons, companies, or entities.

The Contractor grants Caltrans and the FHWA a royalty-free, non-exclusive and irrevocable license to reproduce, publish or otherwise use, and to authorize others to use, the work and information contained herein for government purposes.

DISCLAIMER STATEMENT

The research report herein was performed as part of the Advanced Highway Maintenance and Construction Technology Program (AHMCT), within the Department of Mechanical And Aeronautical Engineering at the University of California, Davis and the Division of New Technology and Materials Research at the California Department of Transportation. It is evolutionary and voluntary. It is a cooperative venture of local, state and federal governments and universities.

The contents of this report reflect the views of the author(s) who is (are) responsible for the facts and the accuracy of the data presented herein. The contents do not necessarily reflect the offical views or policies of the STATE OF CALIFORNIA or the FEDERAL HIGHWAY ADMINISTRATION and the UNIVERSITY OF CALIFORNIA. This report does not constitute a standard, specification, or regulation.

Development of an Articulating Robotic Arm for Spray Painting on Roadways

BY

ROBERT HENRY OLSHAUSEN

B. S. (California Polytechnic State University, San Luis Obispo) 1988

THESIS

Submitted in partial satisfaction of the requirements for the degree of

Master of Science

in

Engineering

in the

OFFICE OF GRADUATE STUDIES

of the

UNIVERSITY OF CALIFORNIA

DAVIS

Approved:

Bahram Ravani
Jan G. Velis
_____
Committee in Charge

1996

i

Acknowledgments

I would like to thank my thesis advisor Professor Bahram Ravani at the University of California at Davis for giving me the opportunity to work on this project and suggesting the topic of my thesis. His focused guidance and unending assistance were invaluable.

I would like to give thanks to the fellow members of the BASR team, Waltar Nederbragt, Richard McGrew, Phil Wong, Rich Blank, and Ken Sprott for their helpful insights and sharing their great wealth of experience.

I would also like to thank Professor Steve Velinsky and Dr. James Schaaf for their time and consideration. Without their assistance and helpful recommendations, none of this would have been possible.

I especially want to thank Lisa for her ceaseless non-technical support and offering of refuge from the day to day grind of thesis writing. I also thank my parents, Robert and Elizabeth, for their concern and unending support throughout my life.

Table of Contents

iv

List of Figures

List of Tables

vii

Robert H. Olshausen
September 1996
Engineering

Development of an Articulating Robotic Arm for Spray Painting on Roadways

ABSTRACT

This thesis discusses the conceptual design of the Big Articulating Stenciling Robot (BASR) Arm that is currently under development at the University of California, Davis. This robotic arm is intended to be used to replace manual methods of spray painting words and symbols on roadways. This will eliminate the hazards of exposing maintenance workers to fast moving traffic and flying debris. Automation of this process can vastly improve maintenance worker safety and reduce restriction of highway traffic.

This thesis deals with mechanical design of BASR which is a long reach articulated robotic arm. A novel linkage design using a pantograph mechanism is used in the design of this arm to eliminate the need for carrying actuators at each joint of the robot. The entire system is designed to operate from the back of a maintenance vehicle and does not need any additional mechanisms for stowing or operating it.

viii

CHAPTER 1 - INTRODUCTION

Highway maintenance operations are some of the most dangerous duties performed to keep the highways safe and functional. Between the years 1972 and 1988, in the state of California alone, there were 4800 highway workers seriously injured enough to keep them out of work [1]. The risks are so great that between the years 1972 and 1991 there were 47 deaths of California highway maintenance workers. One such death occurred on July 29, 1992, to a worker painting surveying markers on a section of Highway 14 in Southern California. This was a manual job that requires a worker to exit the vehicle and expose himself to traffic flow. In response to accidents like this, the Advanced Highway Maintenance and Construction Technology (AHMCT) Center at UC Davis has embarked on projects to automate highway maintenance tasks in order to remove the worker from the pavement. This thesis presents a mechanical design that can perform spray painting of words and symbols on the roadbed with the worker inside the vehicle. Accordingly, the Big Articulating Stenciling Robot (BASR), designed and developed as part of this thesis, will greatly reduce the risks to highway maintenance workers.

This thesis presents the mechanical design and development of the robotic arm, not the entire robot. To this end, parts of the robot not included will be mentioned for clarity but not discussed in-depth.

The following document is broken up into five major sections plus appendices. The first chapter will introduce the current methods for roadway stenciling that are currently in use. Additionally, this chapter will detail the objectives of the thesis. The
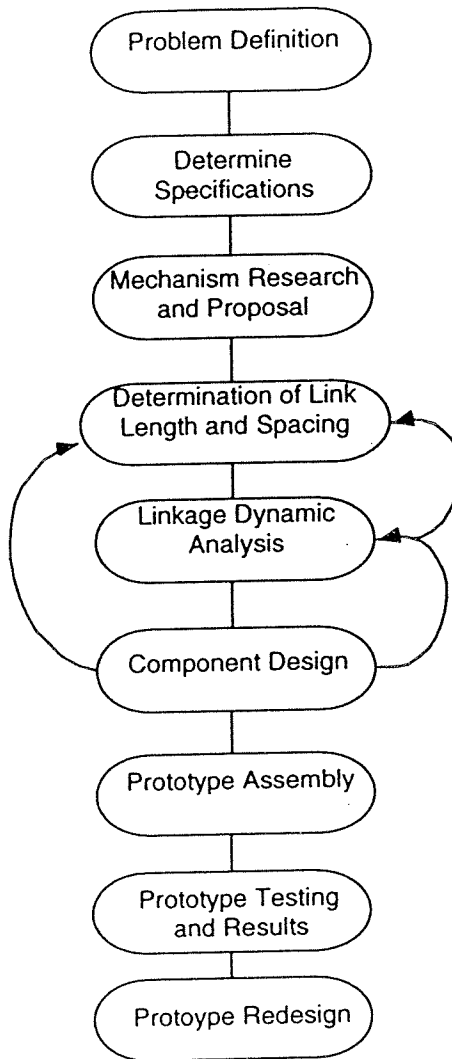
Figure 1.1 *Big Articulating Stenciling Arm Design Flowchart*

second chapter will cover the development of functional specifications and give a general description of the BASR. Chapter three discusses the researching of different configurations for the BASR arm and the acceptance of the final design. Chapter four covers the detailed design, assembly, testing, and modification of the BASR arm. Finally, the last chapter discusses conclusions and recommendations of the project. Figure 1.1 shows the overall design flow chart.

1.1 Literature Search

After a lengthy search, only two other stenciling robots were found to exist. One was created here at the Advanced Highway Maintenance and Construction Technology (AHMCT) Center and the other was created by the Pavement Marking Technologies. They both use gantry type robots to move the end-effector through the painting path. The configurations are discussed below.

The stenciling robot created by AHMCT was designed specifically for painting the aerial surveying premarks [2]. The premarks are 1.2 m x 1.2 m (4ft x 4ft) square and all features of the mark are in a straight line. The premark has a black background with white foreground. An example of a surveying premark is shown in Figure 1.2. This type of mark is ideal for the gantry configuration due to the smaller mark which is much narrower than the 2.4m (8.0 ft) vehicle width. The robot is housed inside a trailer along with its support equipment. The Stenciling Trailer is shown in Figure 1.3.
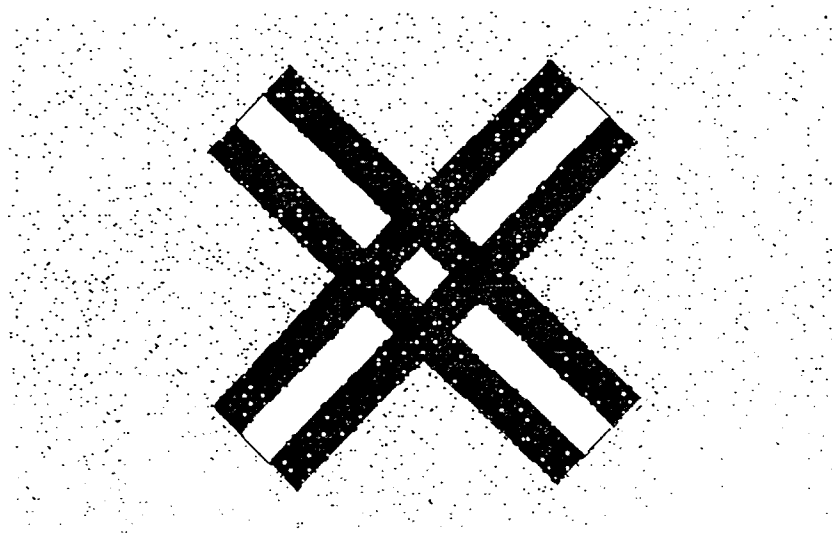
Figure 1.2 *Example of an Aerial Premark*
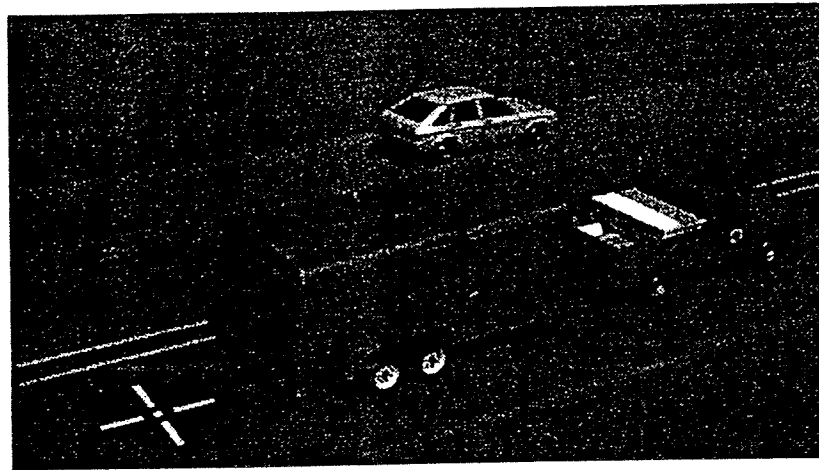
Figure 1.3 *AHMCT's pre-existing Stenciling Trailer*

The stenciling robot developed by Pavement Marking Technologies is designed to spray paint words and symbols on the roadbed. Horizontal positioning of the paint head is controlled by the gantry. Elevation and orientation of the end effector are controlled by a linear positioner and rotary positioner respectfully. All motivation power is electric. The frame of the gantry extends outside of the workspace due to the use of a gantry type robot [3].

1.2 Current In-Use Spray Painting Methods

Many different words and symbols are painted on the roadbed to warn or inform drivers of upcoming events. These words and symbols have a limited life due to vehicular traffic and weather and must be periodically replaced or painted over. To do this, the maintenance worker lays down a stencil of the symbol on the roadbed, aligns it with the existing deteriorated symbol, and then either sprays paint or lays a liquid

thermoplastic material over the stencil. The stencil is then removed and the media is allowed to dry. An example of replacement using thermoplastic is shown in Figure 1.4. The area remains coned off until the media is dry enough to resist automobile traffic. This operation is currently performed by a 2 person crew in one to two vehicles. One vehicle must carry a wide variety and size of stencils in order to maintain the wide variety and size of words and symbols on the highway.
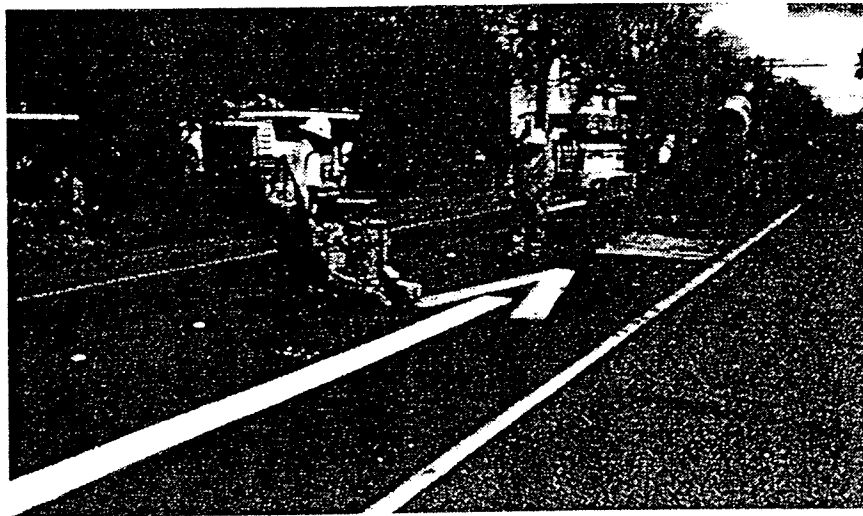
Figure 1.4 *Example of Arrow Replacement Using Thermoplastic Material*

1.3 Problem Description and Objectives

The purpose of this project is to develop a robotic arm to aid in the automation of highway maintenance, specifically the painting of words and symbols on the roadbed. This arm will be designed around a set of specifications which will be defined in Chapter 2. The arm will be designed for static and dynamic loading with sufficient safety factors. Concern will be placed on arm deflection but the arm will not be specifically designed for deflection. Small amounts of deflections will be countered by the active height control incorporated in the end-effector [4]. Numerous tasks performed on the roadway cover a

large workspace requiring a large robot to cover all portions of the workspace. A robotic

arm that can efficiently reach all portions of the workspace and retract into a manageable

size would greatly increase the efficiency of highway maintenance automation.

CHAPTER 2 SPECIFICATIONS OF THE BASR-ARM

2.1 Functional Specifications

Specifications for the Big Articulating Stenciling Robot (BASR) Arm were developed to ensure that the majority of words and symbols on the roadbed could be painted with the same or better quality than is currently obtained manually using stencils. Specifications include workspace size, end-effector speed, end-effector maximum weight, arm rigidity, arm stowed envelop, and simplified control laws.

To effectively cover all words and symbols painted on the roadway, the workspace must be large enough so that a majority of words and symbols are included within that workspace. The majority of words and symbols can all be contained within a 3.7 m by 3.7 m (12 ft x 12 ft) workspace. Some symbols, such as the type III direction arrow [5], are 8 m (24 ft) in length, but these marks are much less prevalent than the marks less than 3.7 m (12 ft) in length. Marks larger 3.7 m (12 ft) can be painted with the support truck moving after the first half of the mark has been painted. Figure 2.1 shows the workspace requirements.
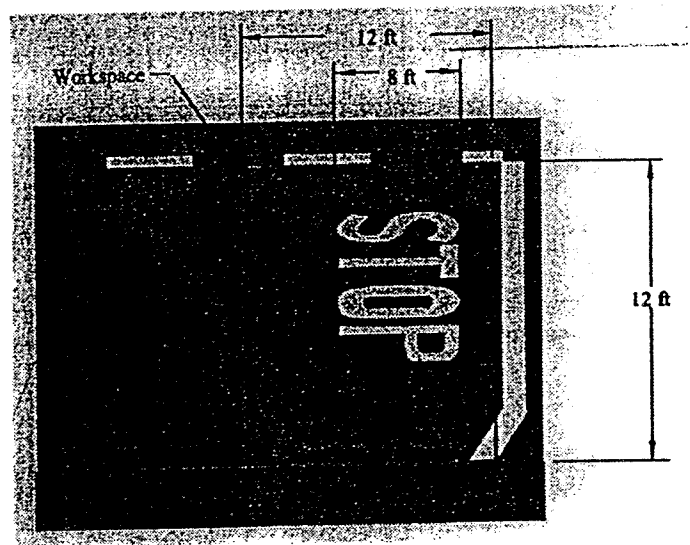
Figure 2.1 *Workspace Requirements*

Painting of words and figures on the roadway is done by high pressure (20.6 MPa or 3000 psi) paint spraying out of an airless nozzle. Tests show that the necessary spray head velocity is approximately 0.3 m/sec (1 ft/sec) with an acceleration of 2 m/sec^2 (6 ft/sec^2) [6]. Therefore, the BASR Arm must be designed to meet these speeds and accelerations from a structural standpoint.

The BASR Arm will be mounted on a support truck and that truck will need to conform with maximum vehicle dimensions. According to the California vehicle codes, standard vehicles must be no wider that 2.4 m (8 ft) and no higher than 4.3 m (14 ft) [5]. The arm can extend from the maximum dimensions when it is in use but must be within these dimensions when stowed. It is desired, but not required that the arm not need any special stowage and handling equipment. Stowing must be performed automatically without the operator exiting the support vehicle.

At the time the specifications were written, the spray painting end-effector had not yet been designed and a weight had not been determined. Therefore, it was estimated that the end-effector would weigh 890 N (200 lbf).

2.2 General Descriptions of the Big Articulated Stenciling Robot

In order to perform the desired spray painting tasks, the robot needs much more than an arm. Much support equipment and structures must be developed and constructed. The BASR is made up of a power unit which provides air, DC and AC voltage and hydraulics for the robot and support systems. The paint is provided by a hydraulically powered positive displacement Binks paint pump. Only one color of paint will be needed since all marks are only painted with one color. Reflective glass beads are provided to the end-effector by placing them under a blanket of compressed air. The end-effector will spray the paint and beads and is capable of three degrees of freedom [4]. The end-effector also has the ability to for active height control. All of the support equipment is mounted in the back of the support vehicle, a flat bed pickup truck. The arm can be mounted on either the front or the back depending on the needs of the local maintenance yard. The support vehicle has front and rear stabilizers to prevent the truck from moving when the robotic arm is moving due to the flexibility in the vehicles suspension. Figure 2.2 shows a sketch of the completed stenciling truck. As discussed in the Introduction (Chapter 1), this thesis presents the mechanical design and development of the robotic arm, not the support equipment and support structures.
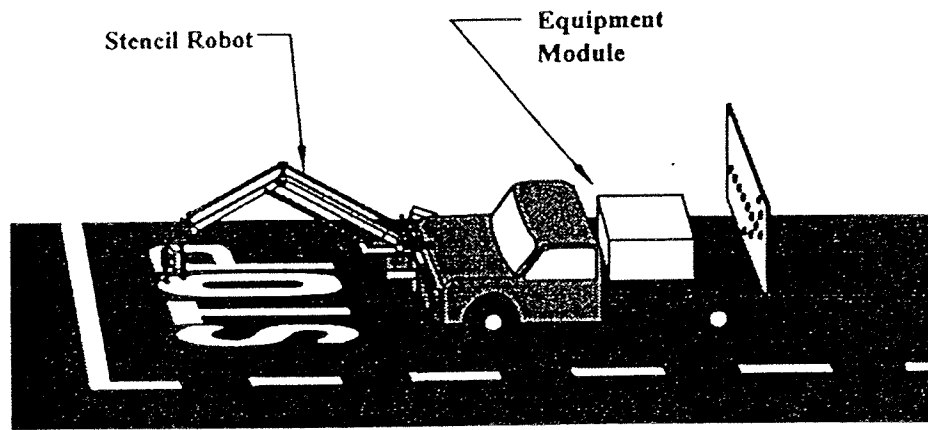
Figure 2.2 *Figure of the Completed Stenciling Truck*

CHAPTER 3 MECHANISM RESEARCH AND PROPOSAL

3.1 Mechanism Research and Configuration Benefits

There were three different configurations considered for the BASR arm. Because of the weight, workspace and speed requirements, gantry, backhoe, and the pantograph types were considered. The following section discusses the each type of configuration and goes over the disadvantages and advantages of each configuration. All of the advantages and disadvantages are summarized in Table 3.1 near the end of this chapter.

3.1.1 Gantry Configuration

This configuration would use two sets of powered linear slides oriented perpendicular to each other. The linear slides would make up a frame around the workspace with the end-effector inside the frame. Figure 3.1 shows the typical gantry configuration. The linear slides can be powered by electric or hydraulic motors. This type of configurations provides for simple reverse kinematics and good position accuracy [3]. Additionally, the end-effector would not need any mechanism to maintain a vertical orientation. The downfall is that the gantry frame must extend outside the workspace, making the frame greater than both the maximum vehicle width (2.4 m or 8 ft) and maximum lane width (3.7m or 12 ft). During transportation, a complex folding mechanism could be employed to reduce the gantry width less than the maximum vehicle width but the gantry would still be wider than the lane width during the painting operation. The large gantry size causes problems with transportation and stowage.
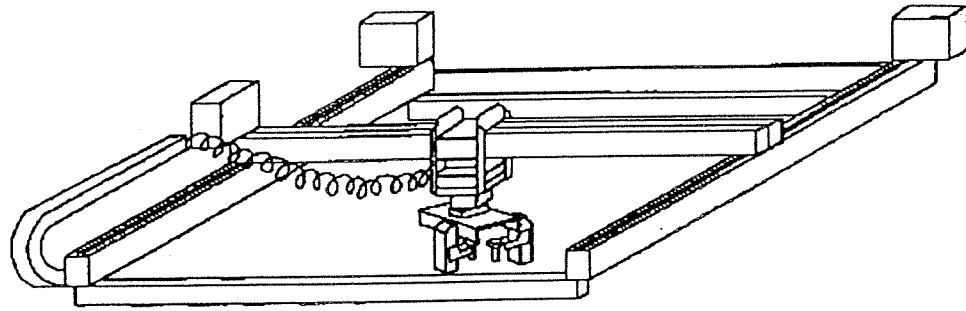
Figure 3.1 *Typical Gantry Frame Configuration*

3.1.2 Backhoe Configuration

The backhoe type mechanism is a familiar sight at many highway maintenance or construction sights. The backhoe operates in the radial coordinate system, thus making the reverse kinematics more complicated than with the gantry configuration. Figure 3.2 shows the typical backhoe configuration. Rotation is accomplished by a revolving base which could be powered by a hydraulic rotary actuator. Displacement is accomplished by a shoulder and a elbow joint. Rotation of these joints would provide for the radial displacement and be accomplished by two hydraulic linear cylinders or rotary hydraulic actuators, one of which must be placed at the elbow joint. This arrangement does not provide for straight line motion at the end-effector within the plane of the workspace. Rotation of both shoulder and elbow joints must be closely coordinated through position sensing and fine position control for straight line motion at the end-effector. This coordination must be carried out by the controller which complicates the control scheme. Additionally, this method requires an actuator at the end-effector to maintain proper end-effector orientation with respect to the workplane. The backhoe does yield a proven mechanical design that is popular in the manual control arena.

Painting Apparatus

Note: All actuators are rotatory actuators.
Note: Each link 8 feet in length

Linear Slide

Truck Mount Point
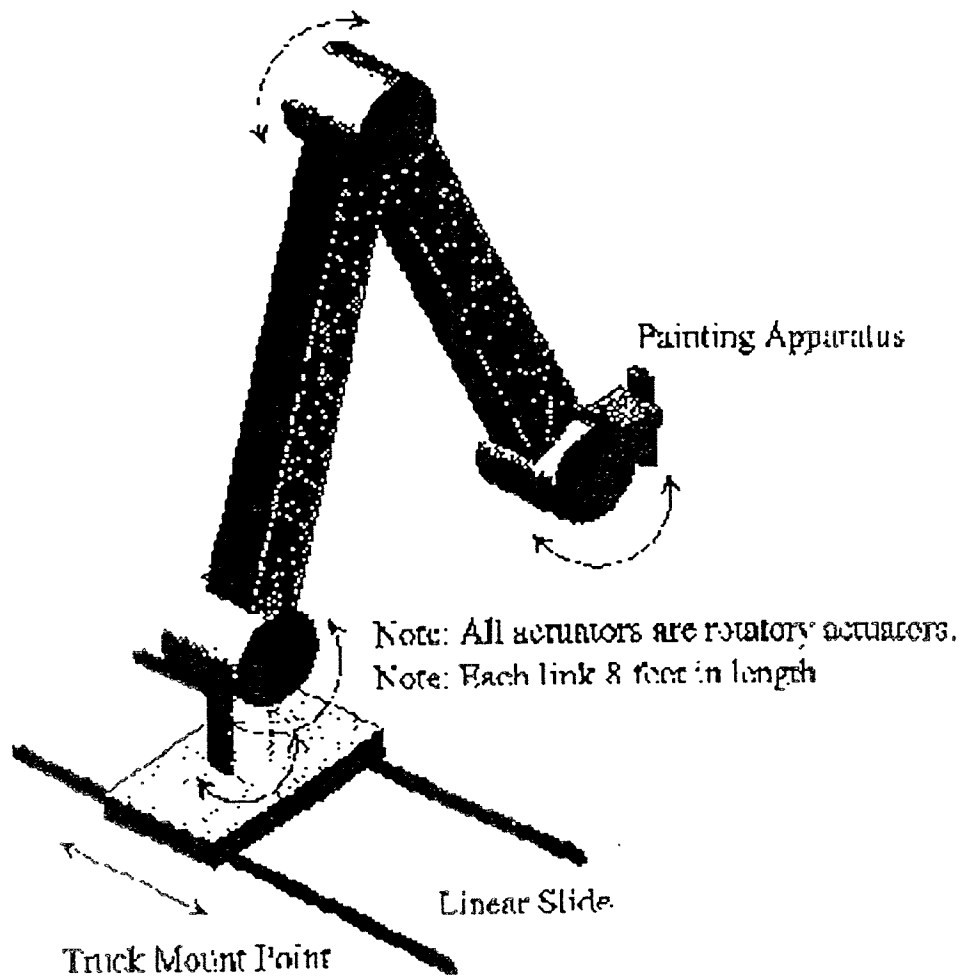
Figure 3.2 *Typical Backhoe Configuration*

3.1.3 Pantograph Configuration.

Figure 3.3 shows a simple pantograph mechanism. Input motion is applied at joint C and the output (end-effector, joint F) moves following the same path as the input but this motion is scaled depending on the linkage configuration (see Section 4.1.1). If

the input is constrained to move in straight line motion, then the output must also move in a straight line motion greatly simplifying the reverse kinematics of the robot [7]. A pantograph robot would use radial coordinates. The workspace coverage is shown in Figure 3.4. The base could be rotated by a hydraulic rotary actuator similar to the backhoe configuration. Unlike the backhoe configuration, the pantograph would only need one hydraulic linear actuator which could be located at the base to reduce the moment caused by its weight and reducing the radial inertia. Since the arm is articulating, it can reach long distances and then fold up to a small package in its stowed position, as shown in Figure 3.3. In order to give the straight line motion and constant ratio of output to input, the pantograph mechanism must be made to close tolerances which could increase productions costs.
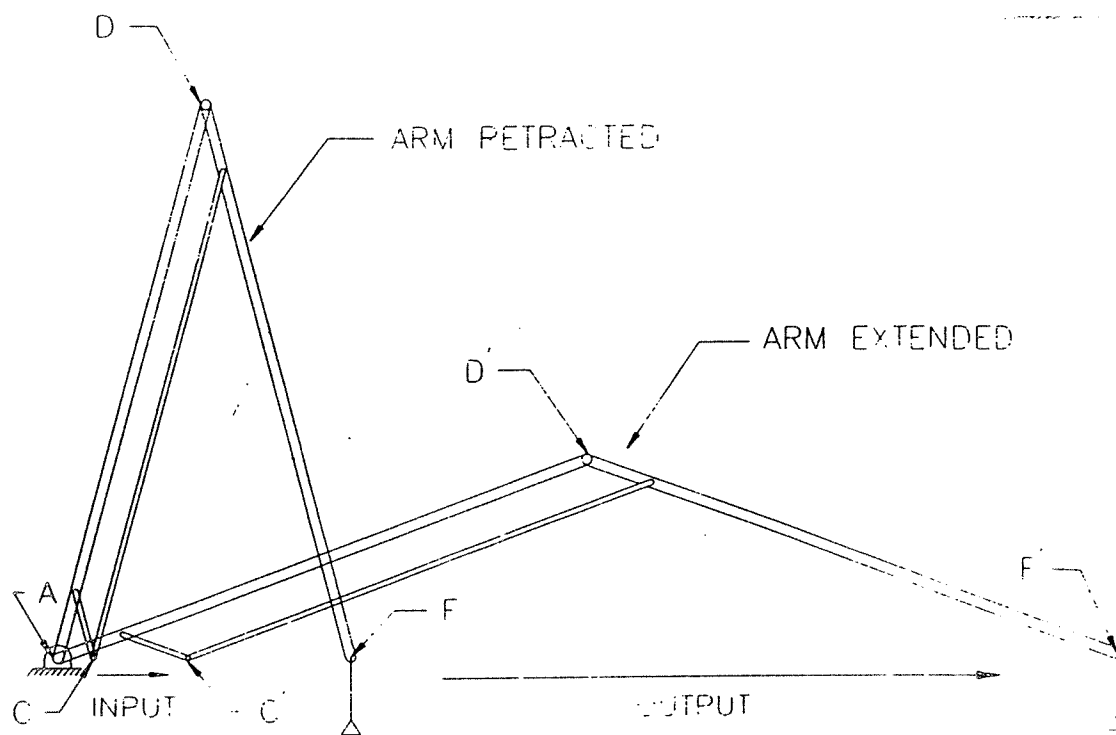
Figure 3.3 *Explanation of Simple Pantographic Motion*
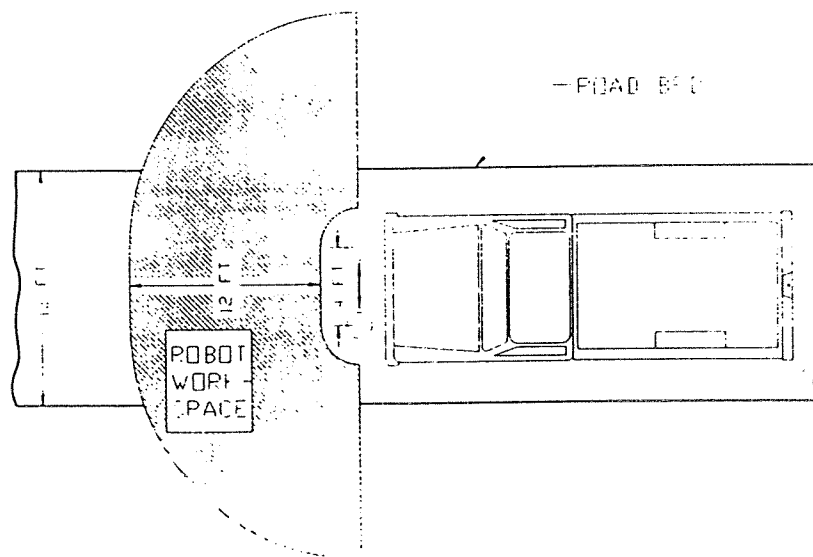
Figure 3.4 *Workspace Coverage with a Pantograph Arm*

To summarize the advantages and disadvantages of each configurations, they are listed in Table 3.1.

Configuration Type	Mechanism Advantage	Mechanism Disadvantage
Gantry	-Linear motion -Simple reverse kinematics -Low height	-Frame is too large to fit in traffic lane -Requires complex stowage mechanism
Backhoe	-Mechanically proven design -Drivers passing by on the road are familiar with the backhoe shape	-Non-linear motion -Difficult reverse kinematics -Elbow actuator not at base -Requires actuator to maintain end-effector orientation
Pantograph	-Linear motion -Simple reverse kinematics -Stowes into small package -All actuators located at base -Simple mechanical linkage provides end-effector orientation	-Tall structure -Not a normal structure

Table 3.1 *Advantages and Disadvantages of Each Arm Configuration*

3.2 Configuration Proposal and Acceptance

On November 30, 1994, the different configurations were presented to the California Department of Transportation (Caltrans). The relative merits and disadvantages of each configuration were discussed and it was decided that the pantograph configuration would be accepted [8].

CHAPTER 4 PROTOTYPE DESIGN AND ANALYSIS

4.1 Component Design and Analysis

Once the general configuration of the BASR arm was determined, detailed design of the prototype could begin. The detailed design started with determination of the main link lengths but the design was an iterative process (reference BASR Design Flowchart, Figure 1.1). With a chosen link length, the resultant forces had to be calculated and then checked to see if they were acceptable. If not, the lengths had to be changed. Additionally, stresses in the links had to be checked when the component design was in process. If the stresses were unacceptable, either the component or the link length had to be changed, adding another iteration to the design process. The following sections show each step of this iterative process.

For reference, Figure 4.1 shows the general configuration of the arm with the letter designations given to each joint.
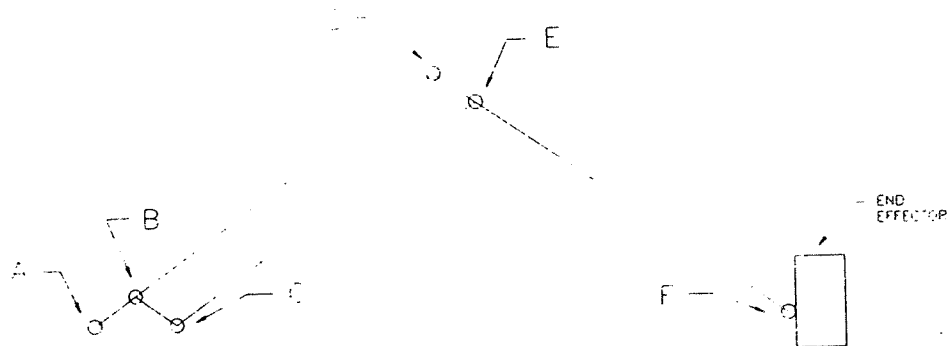
Figure 4.1 *General Arm Configuration with Joints Labeled*

4.1.1 Determination of Linkage Length and Spacing

In order for the BASR arm to reach all areas within the workspace, the arm rotates and extends as discussed in Section 3.1.3. To further enlarge the workspace without requiring a larger arm, the base of the arm can translate 61 cm (2 ft) perpendicular the support truck centerline. Figure 4.2 shows the increase in workspace coverage with and without a translating base. The translating base also helps in stowage of the arm. Stowage of the arm will be discussed in section 4.4.2.
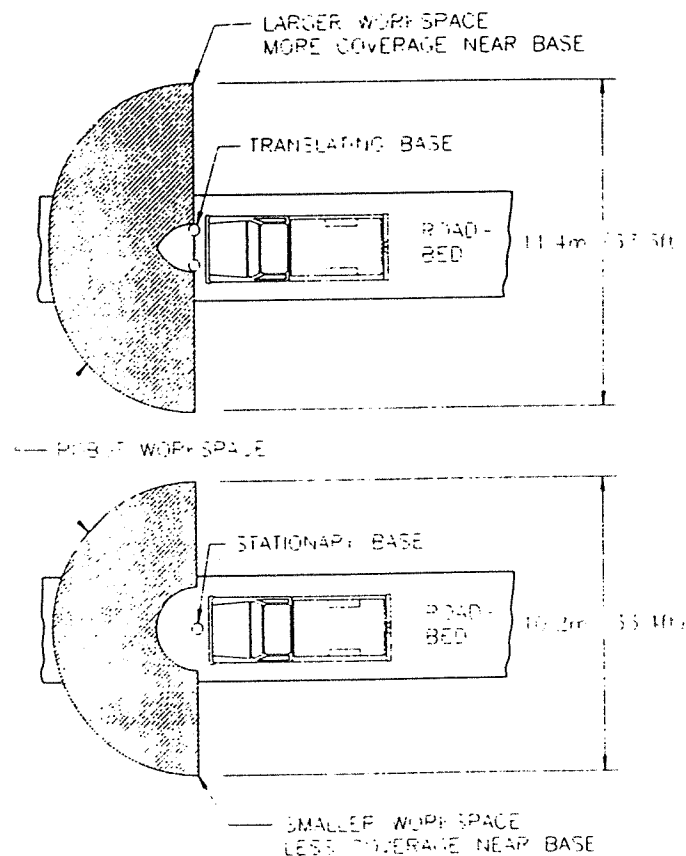
Figure 4.2 *Robotic Reach With and Without Translating Base*

Determination of link length was an iterative process. The Arm is restricted from retracting beyond a minimum angle. This restriction is caused by the interaction between

the links, joints, and hydraulic cylinder. Experiments with different configurations showed that the Arm should retract no less than 15° from vertical. This angle is defined as θ_{min}. With θ_{min} known, the minimum retracted distance can be determined depending on the length of links ABD and DEF. This distance is defined as X_{min}. From X_{min}, the Arm must be able to extend out to the farthest corner of the workspace. This distance is defined as X_{max}. Figures 4.3 and 4.4 help define these terms.
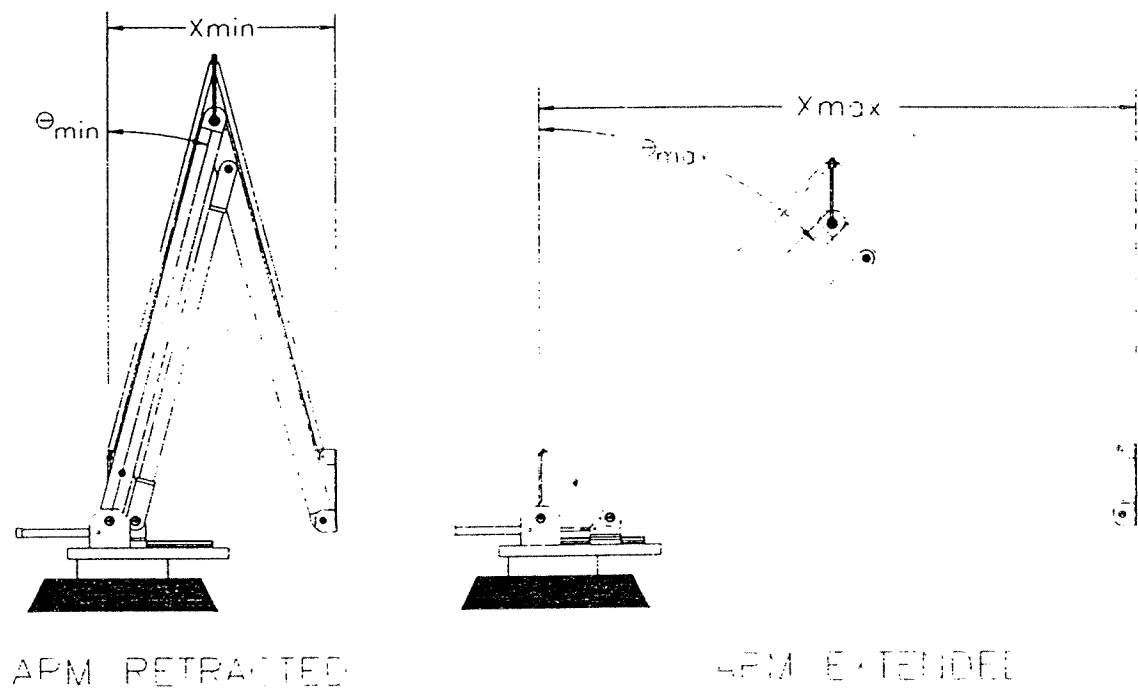
Figure 4.3 *Explanation of Extension and Retraction in Terms of X and* θ
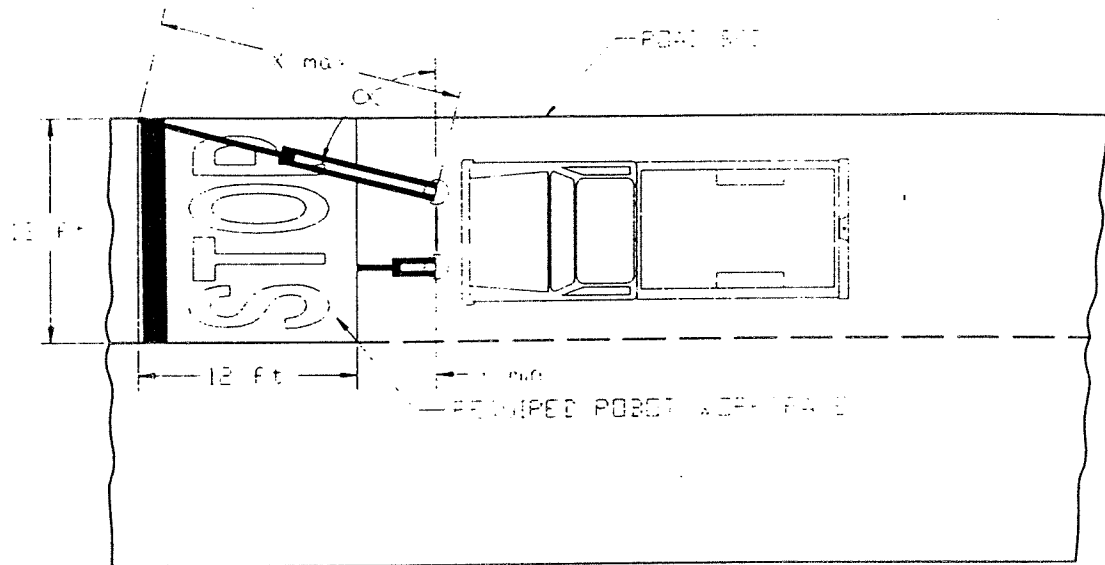
Figure 4.4 *Explanation of Minimum and Maximum Arm Extension in Terms of X and* α

Using these relationships, θ_{max} can be determined for a given length of link ABD and DEF. Iterating through with different link lengths, θ_{max} can be examined to determine the acceptable values for θ_{max} and length of links ABD and DEF. This iterative process is shown on Table 4.1. The term #NUM! in the Theta Max column means that the value can not be calculated. In this case, the arm can not reach all areas within the workspace. The column Max Height is the vertical height of the robot arm in the maximum retracted position ($\theta=15°$).

Theta Minimum (deg)	15.00	0.26	(rads)		
Workspace Width (feet)	12.00	144.00	(inches)		
Workspace Length (feet)	12.00	144.00	(inches)		
Link Length (inches)	X min	X max	Theta Max	Alpha Max	Max Height
101	52.28	202.41	#NUM!	52.85	97.56
102	52.80	202.89	84.03	52.58	98.52
103	53.32	203.38	80.85	52.31	99.49
104	53.83	203.87	78.56	52.04	100.46
105	54.35	204.35	76.68	51.77	101.42
106	54.87	204.84	75.07	51.51	102.39
107	55.39	205.33	73.63	51.25	103.35
108	55.90	205.82	72.34	50.99	104.32
109	56.42	206.30	71.15	50.73	105.29
110	56.94	206.79	70.04	50.47	106.25
111	57.46	207.28	69.02	50.22	107.22
112	57.98	207.77	68.05	49.96	108.18
113	58.49	208.26	67.14	49.71	109.15
114	59.01	208.74	66.28	49.46	110.12
115	59.53	209.23	65.47	49.21	111.08
116	60.05	209.72	64.69	48.97	112.05
117	60.56	210.21	63.94	48.73	113.01
118	61.08	210.70	63.23	48.48	113.98
119	61.60	211.19	62.54	48.24	114.95
120	62.12	211.68	61.88	48.01	115.91
121	62.63	212.17	61.25	47.77	116.88

Table 4.1 *Determination of Link ABD and DEF Length and θ_{max}*

From this data it can be seen that the main links (link ABD and DEF) must be at least 2.60 m (102 in) long in order to reach all areas within the workspace. However, at that link length, the robot arm is nearly horizontal (θ_{max} is 84°, 6° from horizontal). This is not acceptable because the forces in the links and joints would be far too great that close to the horizontal. Table 4.2 shows the forces in the links, joints and hydraulic actuator (F_{act}) if the links are allowed to extend close to the horizontal. Notice the forces at E, D and C at an angle of 85° (5° from horizontal). Appendix A explains the symbology used in Table 4.2.

FORCE CALCULATIONS AT EACH JOINT											
CONSTANTS:			(feet)		(slugs)		(pounds)	-----	(slugs*ft^2)		
		Ra=	4.34	Mabd=	6.24	Wabd=	201.26	Iabd=	78.64		
		Rb=	3.24	Mce=	2.37	Wce=	76.35	Ice=	20.41		
		Rc=	3.63	Mdef=	3.12	Wdef=	100.63	Idef=	39.32		
		Rd=	4.83	Meff=	6.21	Weff=	200.00				
		Rd1=	4.34								
		Re=	4.43			VARIABLE:		(ft/sec^2)		(ft/sec)	
		Re1=	3.24				Aeff=	6.00	Veff=	0.00	
		Rf=	4.83								
		Rlink=	9.17								

THETA	Fex	Fey	Fdx	Fdy	Fcx	Fcy	Fbc	Fax	Fay	Fact	Fnormal
(deg)	(pounds)	(pounds)	(pounds)	(pounds)	(pounds)	(pounds)	(pounds)	(pounds)	(pounds)	(pounds)	(pounds)
15.00	467.46	1722.46	416.41	1423.15	471.98	1798.06	443.34	-292.80	1853.76	-357.24	2226.29
20.00	567.86	1535.33	516.80	1236.49	572.38	1610.65	716.16	-263.00	1912.69	-327.44	2283.62
25.00	674.76	1420.60	623.71	1122.27	679.28	1495.64	905.20	-232.29	1946.80	-296.73	2316.03
30.00	790.64	1342.01	739.59	1044.23	795.17	1416.73	1061.04	-200.21	1968.23	-264.65	2335.62
35.00	918.71	1283.99	867.66	986.81	923.23	1358.36	1207.46	-166.23	1982.10	-230.67	2347.45
40.00	1063.31	1238.73	1012.26	942.23	1067.84	1312.71	1359.18	-129.74	1990.86	-194.17	2353.91
45.00	1230.59	1201.88	1179.54	906.18	1235.12	1275.41	1528.29	-90.02	1995.70	-154.46	2356.07
50.00	1429.62	1170.80	1378.57	876.05	1434.14	1243.79	1727.62	-46.28	1997.10	-110.71	2354.28
55.00	1674.48	1143.77	1623.43	850.18	1679.01	1216.10	1973.80	2.27	1994.96	-62.16	2348.22
60.00	1988.46	1119.60	1937.41	827.51	1992.98	1191.07	2291.51	55.96	1988.61	-8.48	2336.82
65.00	2413.14	1097.36	2362.08	807.30	2417.66	1167.66	2721.29	113.11	1976.37	48.67	2317.73
70.00	3030.96	1076.23	2979.91	789.15	3035.48	1144.84	3336.31	164.06	1954.58	99.63	2285.92
75.00	4032.09	1055.23	3981.04	772.99	4036.62	1121.06	4282.12	164.03	1914.36	99.59	2229.35
80.00	5976.04	1032.36	5924.98	759.68	5980.56	1092.72	5866.89	138.36	1828.72	202.80	2111.50
85.00	11530.65	999.23	11479.60	754.94	11535.17	1043.36	8094.65	3406.89	1561.72	3471.33	1748.86

Table 4.2 *Forces in the Links and Joints When Arm is Extended Past 70°*

If the link lengths were 2.79 m (110 in) then the arm would only extend down to 70° from vertical which yields acceptable forces. Link ABD and DEF will be 2.79 m (110 in) in length. It should be noted at this point that without the translating base the main link lengths would have to be at least 3.05 m (120 in), a 10% increase in length.

The length of the shorter links, link AB, BC and DE can now be determined. While the main links define the reach of the robot, the relationship between longer and shorter links define the amplification factor (output/input) of the pantograph mechanism [7]. When joint A is pinned and joint C (refer to Figure 4.1) is allowed to translate, joint F will translate a distance according to the following linear relationship:

$$OUTPUT = INPUT\frac{LENGTH\ AD}{LENGTH\ AB}\ \text{or,} \tag{1}$$

$$AMPLIFICATION\ FACTOR = \frac{OUTPUT}{INPUT} = \frac{LENGTH\ AD}{LENGTH\ AB}. \tag{2}$$

It would be ideal to have a very high amplification factor. To accomplish this, the short links (link AB, BC and DE) must be much shorter than main link. Unfortunately there is a limit to how small the short links may be made. If the short links are made too small, the spacing between the parallel links ABD and CE will be too small when fully retracted and extended, causing interference between the links. Figure 4.3 shows the arm fully retracted and it can be seen if the arm was retracted any further, that link ABD and CE would interfere. The short links must be big enough to allow for spacing and provide for an adequate amplification. If the amplification factor is not high enough, a long stroke hydraulic cylinder must be used to provide actuation over the required travel of joint C. Table 4.3 shows the trade off parameters for the determination of the short link length.

Short Link Length cm (in)	Amplification Factor	Required Hydraulic Cylinder Stroke for X_{min} cm (in)	Acceptable Clearance Between Links YES/NO?
25.4 (10.0)	11.0	33.3 (13.1)	NO
27.9 (11.0)	10.0	36.6 (14.4)	NO
30.5 (12.0)	9.17	39.9 (15.8)	NO
33.5 (13.2)	8.33	42.9 (17.3)	YES
35.6 (14.0)	7.86	46.6 (18.3)	YES
38.1 (15.0)	7.33	49.9 (19.6)	YES

Table 4.3 *Determination of Link AB, BC, and DE Length*

From the information provided from Table 4.2, it was determined that the correct length for the small links (links AB, BC and DE) would be 33.53 cm (13.20 in) providing for an amplification factor of 8.33.

4.1. 2 Linkage Dynamic Analysis

With the length of each link known and the specifications for workspace, end-effector speed and acceleration, and end-effector weight known, the forces in each link can be found. To determine these forces, equilibrium equations were written for each link resulting in twelve linear equations with twelve unknown variables. The equations were solved for a given end-effector weight, acceleration and velocity while varying end-effector position. The resultant forces in each link and joint were calculated along with the maximum stresses in each link. The free body diagrams, equations and spread sheets

containing the data are shown in detail in Appendix A. It is easily seen that the maximum

forces are caused at the maximum extension of the arm, so all links must be designed

with these values as worst case. The maximum stress in each critical position are shown

in Table 4.4.

Critical Location	Stress Mpa (psi)	Arm Position	Arm Dynamics in/sec² (ft/sec²)
Link ABD Joint B	35.53 (5157)	70° (extended)	Accel= -2 (-6) Vel=anything
Link BC	8.082 (1173)	70° (extended)	Accel= -2 (-6) Vel=anything
Link CE	5.953 (864)	70° (extended)	Accel= +2 (+6) Vel=anything
Link DEF Joint E	19.23 (2971)	70° (extended)	Accel= +2 (+6) Vel=anything

Table 4.4 *Maximum Stresses in the Critical Links*

4.1.3 Linkage Type and Configuration

The links must maintain the proper distance between the joints and limit

deflections due to bending stress. Maintaining proper spacing between joints ensures that

the arm will provide output motion that is linear with respect to the input. Additionally,

the proper distance will allow the linkage configuration to remain intact providing for

straight line motion of the end-effector. If the links are allowed to bend or deflect, the

ability of the linkage to provide straight line linear motion will be degraded.

Since link weight was needed to be kept to a minimum, rectangular extruded

aluminum tubes were used. These tubes are one third the weight of steel tubes, with

almost the same strength, 340 MPa (50 kpsi) vs. 275 Mpa (40 kpsi) [9]. The main links

were made up of 10cm x 15cm (4in x 6in) by 6.4mm (0.25in) thick stock.

In order to fasten the shafts or bearing cups-to the tubes, solid aluminum inserts were connected to each end of the links in the area of the joint. These inserts were bonded to the tubes by the use of high strength adhesive made by 3M Corporation. The adhesive was 1838-L B/A Scotch weld two-part epoxy with a 21 Mpa (3.0 kpsi) [10]. Using adhesive to attach the inserts into the tubes precludes the deformation and stresses associated with welding. Additionally, the long set up time of the adhesive (8-12 hours) allows the inserts to be placed in position and then verified for correct position before the adhesive has set.

Link CE was made up of smaller outside dimension tubing since it is the only link, besides link BC, that is in pure compression. The main portion of the link is made up of 10cm x 10cm (4in x 4in) by 6.4mm (0.25in) stock. Link CE also has side arms so that it can mount at joints C and E. Link BC is the shortest link and was made up of solid aluminum for ease of manufacturing.

4.1.4 Joint System

An important part of maintaining the robotic motion linear and repeatable is the pinned joints. Each joint must handle the loading due to the weight of the links and the end-effector while still allowing the joint to rotate with a minimum amount of friction. Also, the joint must be resistant to any displacement or deflection other than rotation it is designed to allow. To meet these requirements, opposed angular contact roller bearings where used [11]. Figure 4.5 shows a typical bearing arrangement.
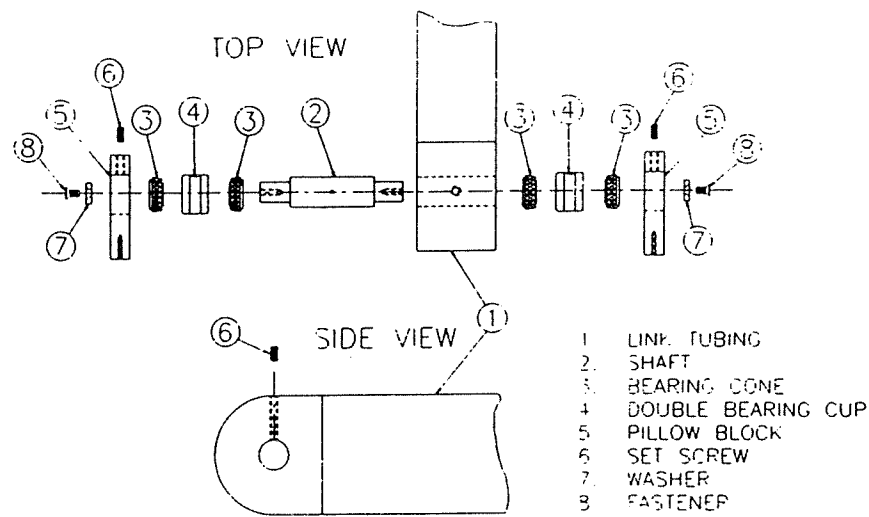
Figure 4.5 *Typical Bearing Arrangement.*

Angular contact roller bearings are able to take both radial and axial loading. In this bearing arrangement, the majority of the loading will come from the pin loading, acting on the bearing in a radial direction. This is consistent with angular contact roller bearing design since angular contact roller bearings are designed to carry the majority of loading in the radial direction[11]. Axial loading of the bearing will come from any side loading and joint preloading. Side loading comes from rotary acceleration or deceleration of the robotic arm, end-effector and payload. Joint preloading is necessary to ensure that there is no play in the joints. Play would allow for displacement of the joints in a direction other than rotation, reducing the placement accuracy of the end-effector.

4.1.5 Linear Slide

Joint C must be constrained to translate in only one degree of freedom in order for the end-effector to maintain its straight line motion. This constraint is obtained by

mounting the shaft at joint C on a carriage of a linear slide assembly. The linear slide would have to be strong enough to withstand the vertical force created by the weight of the linkage and payload at the end-effector. The force was calculated to be 11,800 N (2670 lb). Various linear slides were investigated and a INA KUSE35L linear slide was found to meet these requirements.

Joint C must also provide for an attachment point for the end of the linear hydraulic actuator. The actuator is attached to the pillow block through a pin and rod end system at joint C and a trunion mount at joint A. This allows the cylinder to rotate and align itself due to any shifting or bending in the support which isolates the cylinder from any bending moment which would degrade the seals.

4.1.6 Parallel Mechanism

The use of the pantograph mechanism allows the extension actuator to be mounted at the base saving weight hydraulic lines running out the arm all of the while giving straight line linear motion at the end-effector. This is very advantageous but does not guarantee proper orientation of the end-effector with respect to the road surface. In order to maintain the proper orientation, a mechanical linkage or actuator could be used to maintain the orientation.

If the end-effector was hard mounted directly to link DEF, its orientation with respect to the road surface would change as link DEF rotates as it is extended or retracted. One way to maintain the proper end-effector orientation is to mount an actuator between link DEF and the end-effector mount. The actuator would be given a position command based on the angular displacement of link ABD. This would require more weight at the

end of the arm and more electrical or hydraulic cables to be routed out to the actuator. Additionally, any misalignment caused by the actuator system would cause error in the end-effector.

Another alternative is to use identical gears at joints A, C, and F. The gear at joint A would be fixed to the base while the gears at joints C and F would be free to rotate with respect to the links. If the gears are connected with chains, the gear at joint F would maintain its orientation with respect to the gear at joint A and in doing so, maintain its orientation with respect to the base. The gears and chains are heavy, adding too much weight to the arm. Some weight savings could be achieved by replacing the gears with pulleys and chains with belts. This alternative would still weigh too much and be susceptible to stretching. A better, lighter, and less complex system was needed.

Further research discovered a reliable and simple system to maintain the end-effector orientation. Based on the principle that ends of a parallelogram stay parallel due to the opposite sides being equal length, a linkage mechanism could be mounted above links ABD and DEF to maintain end-effector orientation. Light weight links made of composite materials could be used to save weight and still provide the required strength. No actuation would be necessary since the action of the arm would maintain the position. Figure 4.6 shows the parallel linkage.
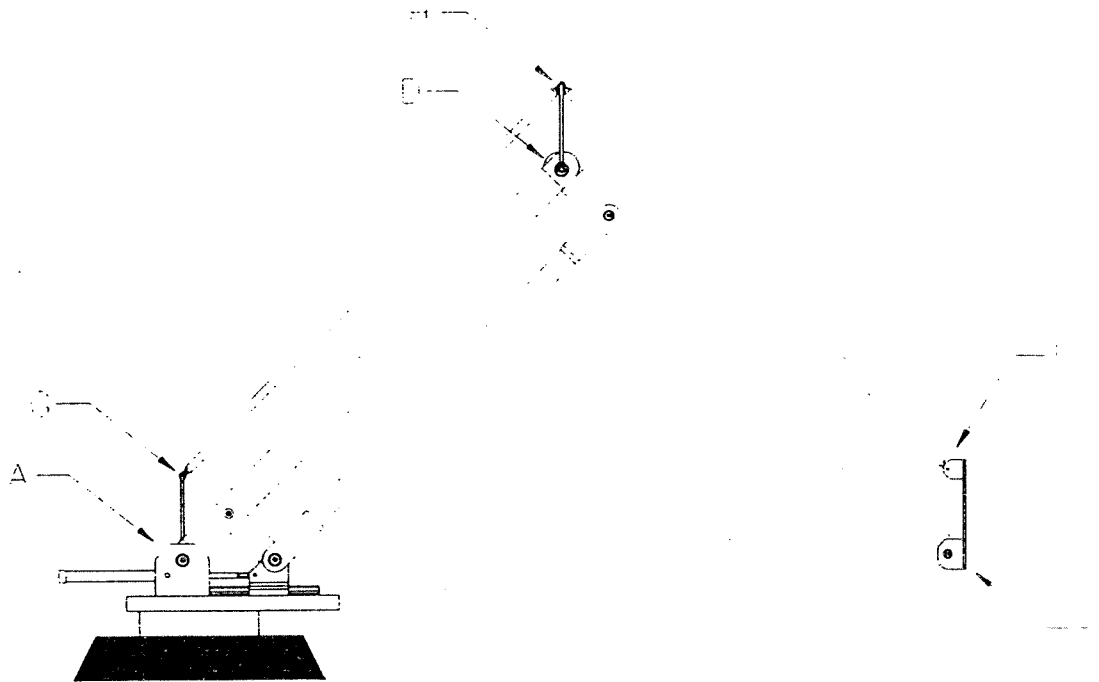
Figure 4.6 *View of the BASR arm with the Parallel Linkage Attached*

The parallel links were made from carbon graphite tubes with aluminum plugs epoxied at both ends. The plugs were drilled and tapped to allow spherical rod ends to be threaded into the plugs. This thread gives minor adjustments in length which is needed when maintaining the links the same length. The shorter links of the parallel linkage parallelogram, links AG, DH, and FI are made up of links 43.18 cm (17.00 in) long. Link AG maintains the orientation of the parallel mechanism and is hard mounted to the inside base pillow blocks. Link DH is mounted to the shaft at joint D but is free to rotate independently of the shaft. This rotation is accomplished by more spherical rod end bearings. The universal end-effector mount provides for the remaining side of the

parallel linkage parallelogram. These parallel links maintain the end-effector in the correct orientation without any control scheme or actuation required.

4.1.7 Universal End-effector Mount

The end-effector is mounted to the end of link DEF through the universal end-effector mount. This mount is made up of 6.4 mm (0.25 in) aluminum plate which is fastened to two sets of pillow blocks. The lower set houses the tapered roller bearings at joint F and the upper set houses the pin for joint I. The plate also provides for spacing of the link FI in the parallel linkage. Four fasteners secure the end-effector to the universal end-effector mount. Figure 4.7 shows the side and front views of the universal end-effector mount.
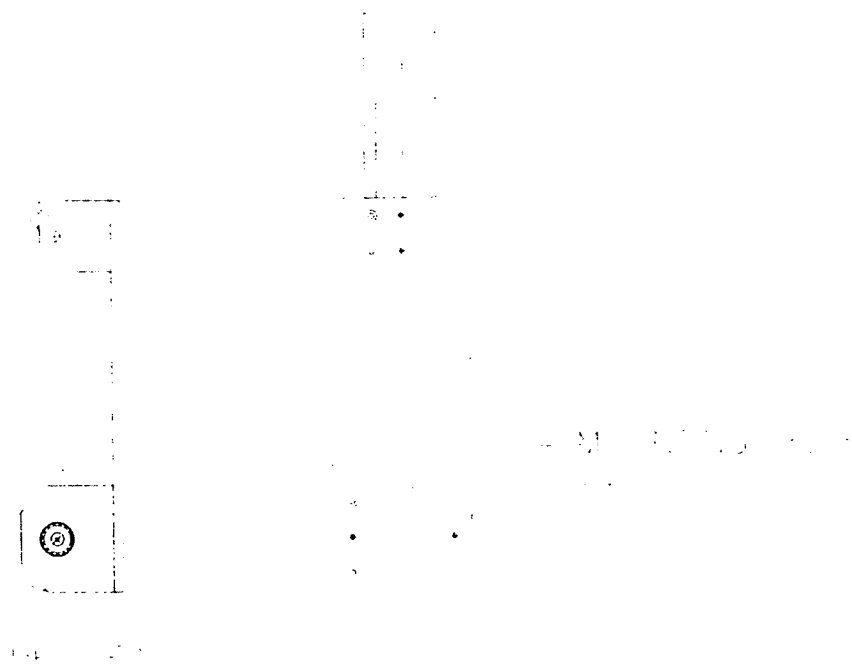
Figure 4.7 *Universal End-Effector Mount*

4.2 Prototype Assembly

The first major parts of the BASR arm to be assembled were the main links. Before the links could be assembled, the bearing cups were pressed into the ABD inserts at joint D. In parallel with this, the aluminum tubes were accurately machined to length in order to provide the correct spacing between joints. Once all of the aluminum tubes were machined to length and the corresponding plugs were completed, tubes and plugs were epoxied and clamped together to form the main links. A jig was used to check and maintain the correct distance between joints.

With the links assembled, the entire Arm could also be assembled. During the first stage, links ABD and DEF were assembled horizontally. The left hand side link ABD was first placed on the turntable bearing interface by securing the link to its pillow blocks (Pillow Block, Joint A) and securing the pillow blocks to the interface. Joint D shaft was fastened to link DEF and then attached to the left hand link ABD through the bearings in Link ABD at joint D. The right hand link ABD was then attached at joints A (by the pillow blocks), B (by the shaft at joint B), and D (by the shaft and bearings). The link was not securely fastened yet because the shaft at joint B had to be slipped through left and right link ABD and the bearings for link BC at joint B. Once the shaft was secured and the tapered roller bearings on link BC at joint B were properly preloaded by shims, the remaining joints on link ABD could be secured.

Before anymore assembly could continue, joint D had to be raised so that the main links were in the normal operating position and then held there until the remaining links and joints were attached. With joint D raised such that link ABD was about 20° from

vertical, joint C and the linear slide could be assembled by slipping the shaft at joint C through the sliding carriage and tapered roller bearings on link BC at joint C. Link CE was then assembled by placing the two side arms on either side of the sliding carriage at joint C and tightening the bolts that secure the joint. The side arms at joint E are placed on the shaft at joint E and then the joint was secured to link DEF. The end plates are secured to the side arms and then the tube between the end plates was secured to the plates which completed link CE and the assembling of the BASR arm.

4.3 Prototype Testing and Results

Once the Arm was assembled, testing to ensure that it met the design requirements could be conducted. At the time of writing this thesis, the Arm had not been actuated under closed loop electronic control. Testing was accomplished using static and some open loop (manual) control.

4.3.1 Arm Deflection Under Design Loading

Deflection of the Arm was tested by incrementally extending the Arm with and without the end-effector payload. To measure deflection, a laser level was shined horizontally from the base interface (joints A and C) onto the end-effector. Any deflection in the Arm was measured by noting the displacement in the laser light beam. The results from the testing are presented in Table 4.5.

Arm Extension meter (ft)	No Load Deflection cm (in)	Full Load Deflection cm (in)
0.30 (1.00)	0 (0)	0.16 (0.063)
0.61 (2.00)	0 (0)	0.48 (0.19)
1.22 (4.00)	0.078 (0.031)	0.40 (0.16)
1.83 (6.00)	0.16 (0.063)	0.64 (0.25)
2.48 (8.00)	0.32 (0.13)	0.80 (0.31)
3.05 (10.00)	0.48 (0.19)	1.51 (0.60)
3.66 (12.00)	0.56 (0.22)	1.91 (0.75)

Table 4.5 *Results from the Arm Deflection Test*

Although the maximum under load deflection was not specified at the conception of this project, the actual deflections fall well within practical limits. The largest deflection recorded was 1.91 cm (0.75 in) which is well within the end-effector's active height control ability.

4.4 Prototype Redesign

Through design, assembly and testing, it was noticed that portions of the design could be modified to improve performance and safety. Some modifications would require significant redesign of the existing prototype design and therefore will be postponed until the second stage prototype is designed. The following modifications will be implemented to the existing prototype to improve performance and safety.

4.4.1 Parallel Linkage Redesign

Originally, the parallel links were placed above links ABD and DEF. This posed a height restriction as the link DH was 43.18 cm (17.00 in) above joint D. See Figure 4.8 for an illustration of the overall height of BASR. If the parallel linkage could be placed below the main links the overall height of BASR could be significantly reduced. It was decided to move the parallel linkage mechanism below the main links.
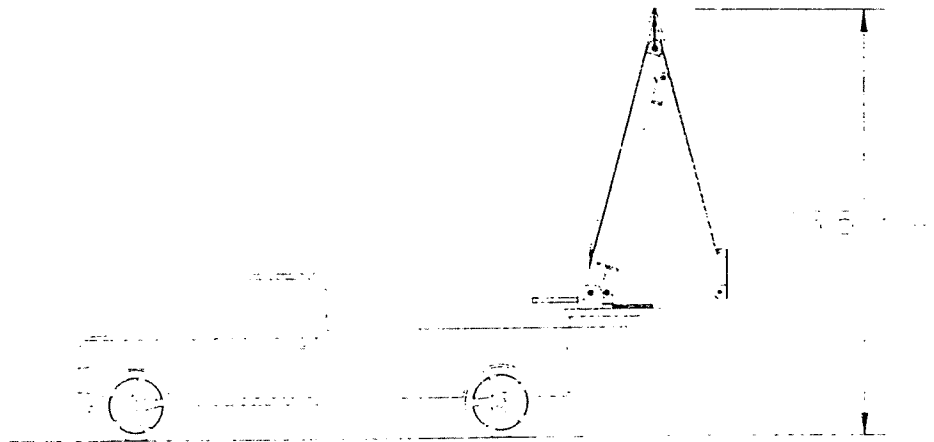
Figure 4.8 *BASR Overall Height with the Arm Retracted*

Joint G was moved from above joint A to below Joint A. The parallel link GH is mounted at joint G 22.84 cm (8.993 in) below joint A on the turntable bearing interface. This is the maximum spacing between joints A and G before the link GH will interfere with the rotating base of the robot. Because of the smaller spacing between the main links and the parallel links, larger tension and compressive forces will be seen in the links therefore two sets of parallel links will be used, one on either side of the main links.

Link DH must be free to rotate around the center of joint D but be constrained from moving in other directions. The shaft at joint D already had a 5/8-16 UNF tapped hole at both ends. If the proper mechanism could be found to use this thread and allow the one degree of freedom (rotation about the axis of joint D), the lower parallel linkage design would be essentially complete. It was found that a cam follower would thread into the threaded joint D and if link DH was pressed onto the bearing surface of the cam follower, the link would be properly constrained. This approach was used with a 1.59 cm bolt passing through joint H and holding links GH and HI. There is no connection between the left and right hand sides of joint H because this connection would interfere with the main links when the arm was retracted towards the stowed position.

There was not much change made to joint I. The universal end-effector mount was rotated so that it was hanging below joint F. The pillow block for joint I were move so that they met the same spacing from joint F as joints A and G were spaced. Since there were two parallel links HI now versus one on centerline, the length of the shaft at joint G had to be lengthened to accommodate the width of the spacing between both links. Figures 4.9 and 4.10 show the final configuration of the parallel linkage mechanism.
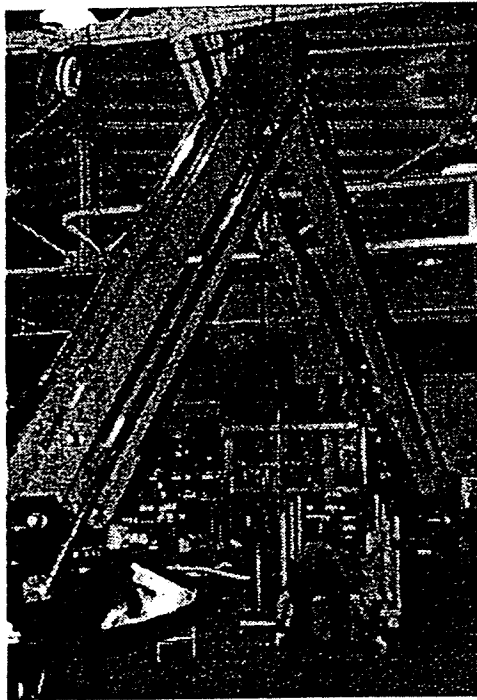
Figure 4.9 *Side View of the Modified Parallel Linkage*
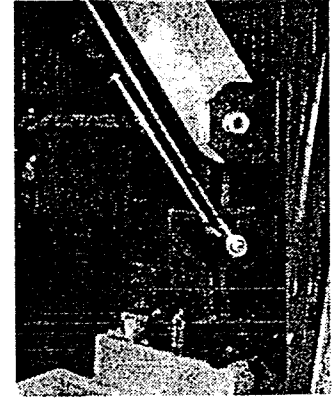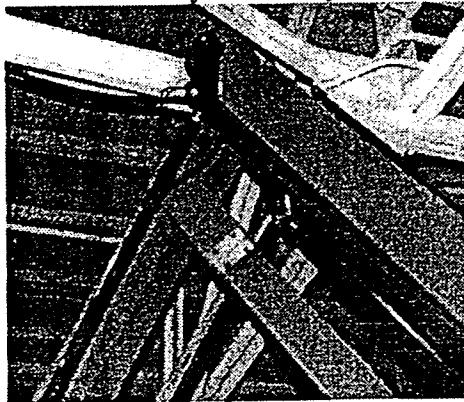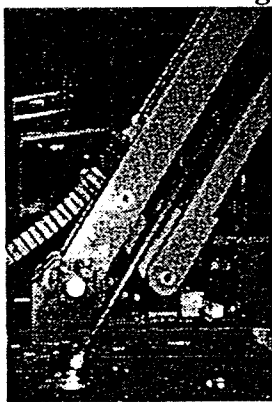
Figure 4.10 *Side View of Base, Joint H, and End-Effector Respectfully*

An added advantage of placing the parallel links below the main links is that the universal end-effector mount is now mounted mostly below joint F. Rotating the mount and mounting it below joint F lowers the center of the universal end-effector mount and therefore also lowering the height above the pavement of the paint head. Additionally, the universal end-effector mount does not have to be as long now that the parallel links

are only spaced 22.84 cm (8.993 in) apart. Shortening the mount from 55.9 cm (22.0 in)

to 27.9 cm (11.0 in) reduces its weight by 50 percent.

4.4.2 End-effector Retraction for Stowage Redesign

It was decided that the BASR arm have the ability to stow the end-effector within

the bed of the support truck. As BASR is transported between work sites, it would be

safer to have the arm rotated around and over the bed of the truck so that it is completely

within the confines of the truck bed and that the paint head is rotated to horizontal so that

it is not in danger of striking objects on the roadway. Different schemes were

investigated for merit. The optimum retraction scheme is shown in Figure 4.11.
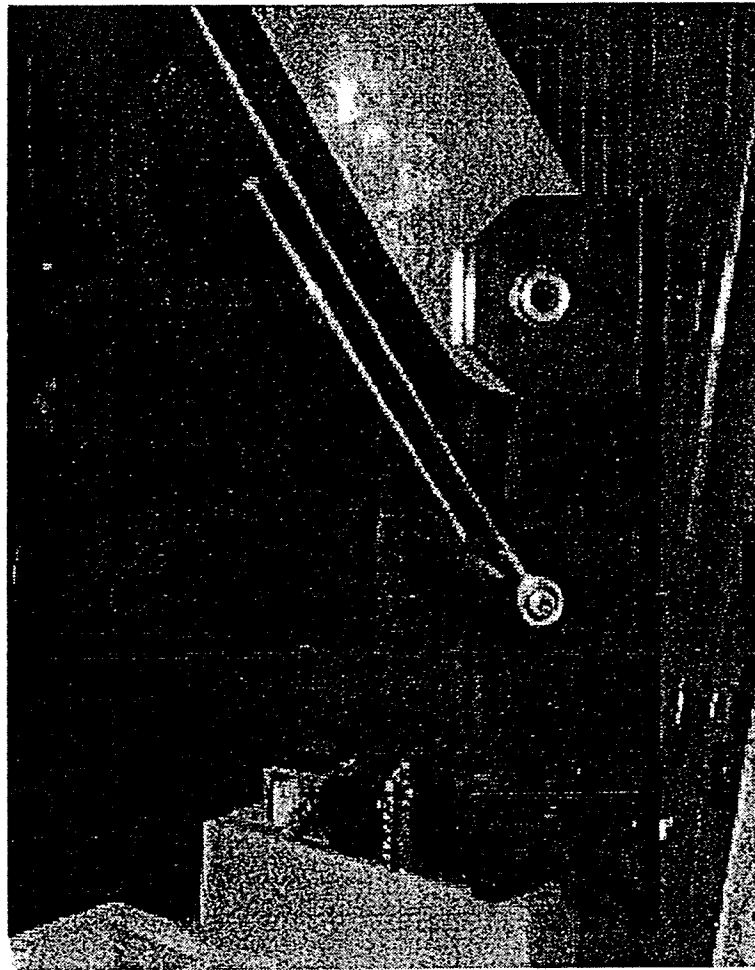
Figure 4.11 *End-effector Retraction Mechanism*

The end-effector is retracted by changing the length of parallel links HI. In the normal working (non-retracted) position, link HI is the original 27.94 m (110 in) length. To rotate and retract the end-effector, link HI shortens 33 cm (13 in). When the end-effector is needed in its working position, the link extends to its original length. This extension and retraction is accomplished by an air cylinders imbedded in the end of the two link HI's. When the cylinder is retracted, the link is short and when the cylinder extends to full stroke, the link expands to its full 27.94 m (110 in) length. The air cylinders are actuated by 1.03 MPa (150 psi) air which was already available to the end-effector. The status of the end-effector rotation is sensed by hall effect switches mounted

on each pneumatic cylinder. When the end-effector is retracted over the truck bed, air to the air cylinders is vented allowing the end-effector to rest in restraints provided in the truck bed.

5 CONCLUSIONS

5.1 Conclusions

This thesis discusses the multiple developmental stages involved in the mechanical design of the Big Articulating Stenciling Robot (BASR) Arm. Current methods and mechanisms used to paint words and symbols on the roadway are presented to establish the direction that was taken towards the generation of overall conceptual designs. The previous chapters include general descriptions of the individual systems that constitute the BASR as well as more detailed descriptions of the BASR Arm. The generation of multiple arm concepts and the impartial trade-off process provide a logical means of selecting the most effective design while identifying the strengths and weaknesses of each design. The development of the Arm as presented in Chapter 4 and Appendix A is also presented to show the step by step process used to design the accepted concept.

5.2 Recommendations

During initial prototype testing, it was determined that the overall arm height above the roadbed while retracted was too tall and should be reduced. Contributing to the overall height was the parallel linkage mechanism. If the mechanism height could be reduced, the overall performance of the arm would be greatly improved. Modifications to the linkage were undertaken and the initial modifications are discussed in Section 4.4.1. Further modifications could improve the parallel linkage even further. Experimentation

with other mechanisms and geometry may yield a parallel linkage extends along link DEF only, eliminating the linkages along link ABD.

Approximately 30 - 40% of the stress in the links and shafts is due to the weight of the links and joint materials. To reduce this contribution to the overall stress, the Arm was made from heat treated aluminum. Although aluminum is lighter than steel, it is not as stiff as steel, lowering the natural frequency of the structure. Alternative materials to aluminum should be investigated to further reduce the weight of the structure while increasing natural frequency of the structure. An alternative material to aluminum is carbon fiber composites.

BIBLIOGRAPHY

[1] Sacramento Bee, *Highway Workers Bill Gains*, Capitol News, February 12, 1990.

[2] Sprott, K. S., Wong, P. W., Nederbragt, W., Olshausen, R., and Ravani, B., *A Description of the Photogrammetery Target Project Premark Painting System*, UCD-ARR-94-09-09-01, UC Davis, CA., 1994.

[3] Long, Elan, *Gantry Robots*, International Encyclopedia of Robotics: Applications and Automation, Volume 1, 579-587, 1988.

[4] McGrew, Richard A., *A Robotic End-Effector for Roadway Stenciling*, Masters Thesis, UC Davis, CA., 1996.

[5] Caltrans, *Standard Plans*, California Department of Transportation, Sacramento, CA, 1988.

[6] Kochiekali, H., Ravani, B., A Feature Based Path Planning System for Robotic Stenciling of Roadway Markings, ASCE Conference on Robotics for Challenging Environments, Albuquerque, NM, 1994, pp. 52-60.

[7] Yang, D. H. C., Lin, Y. Y., *Pantograph Mechanism as a Non-Traditional Manipulator Structure*, Mechanism and Machine Theory, 20(2), 115-122 (1985).

[8] Sprott, K. S., Nederbragt W., Olshausen, R., W., Wong, P. W., and Ravani, B., *General Stenciling Project Preliminary Concepts and Proposals,* UCD, November, 1994.

[9] Shigley, J. E., Mitchell, L. D., *Mechanical Engineering Design, Fourth Edition,* McGraw-Hill, NY, 1983.

[10] 3M, *Designer's Reference Guide to User-Friendly Adhesives for Product Design and Assembly,* 3M Industrial Tape and Specialties Division, St. Paul, MN., 1993.

[11] Timken, *Bearing Selection Handbook Revised - 1986.* Timken Company Engineering Services, Canton, OH., 1984.

APPENDIX A
FORCE, MOMENT, AND STRESS CALCULATIONS
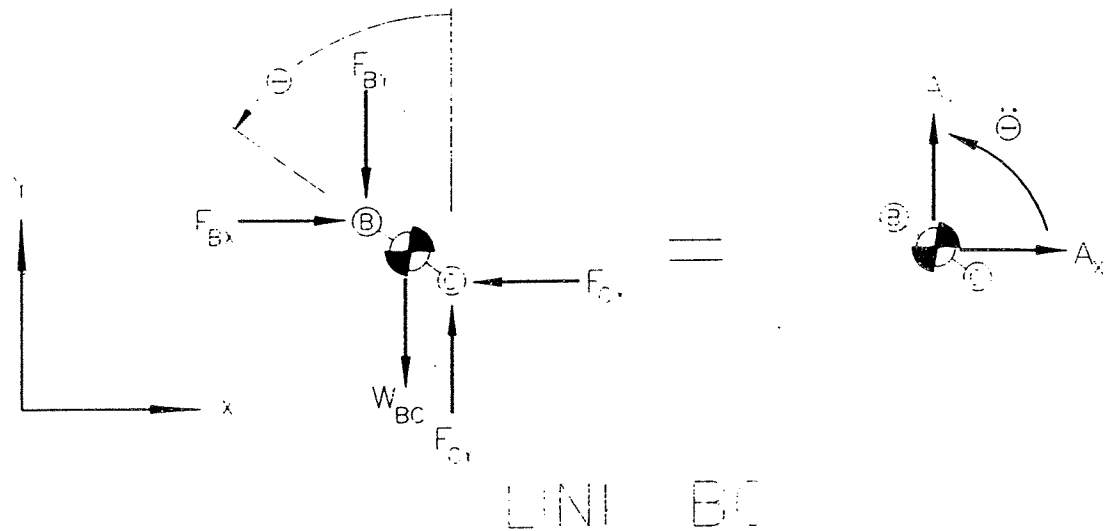
Figure A.1 *Link BC Free Body Diagram*

FORCE IN LINK BC

Assume that link BC is massless (less than 10lbf)

$$\sum F = M_{BC} A = (O)A = 0$$
$$\Rightarrow \sum F = 0, \quad so,$$

(1)

$$\xrightarrow{+} \sum F_X = 0$$
$$F_{BX} - F_{CX} = 0 \quad \Rightarrow \quad F_{BX} = F_{CX}$$

(2)

$$+\uparrow \sum F_Y = 0$$
$$-F_{BY} + F_{CY} = 0 \quad \Rightarrow \quad F_{BY} = F_{CY}$$

Force acts along the link axis and the force is just F_{BC} at angle Θ as shown in Figure A.2.

APPENDIX A
FORCE, MOMENT, AND STRESS CALCULATIONS
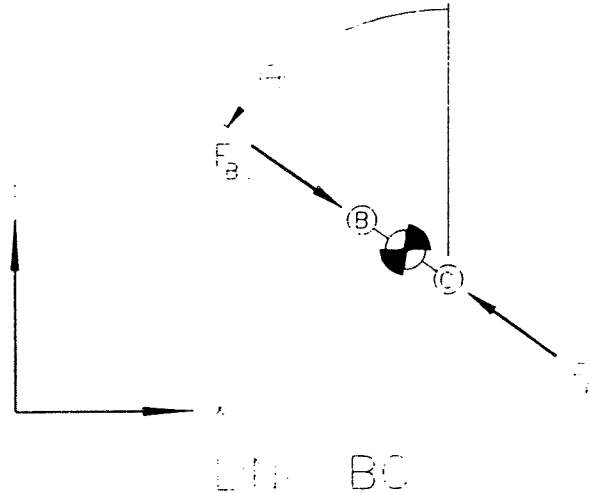
Figure A.2 *Link BC Free Body Diagram Showing Forces in Line with Link*

STRESS IN LINK BC

Since the link is just in compression without any bending moment, determine just compresive stress due to F_{BC}.

$$\sigma_{BC} = \frac{F_{BC}}{A_{BC}} \qquad \text{Where } A_{BC} \equiv \text{Cross sectional area of link BC} \qquad (3)$$

NOTE 1: Cross sectional area of the link is defined as the minimum cross section area minus material removed for the shaft or bearing at that joint.

NOTE 2: In this link, buckling is ignored due to its short length (low L / k).

APPENDIX A
FORCE, MOMENT, AND STRESS CALCULATIONS
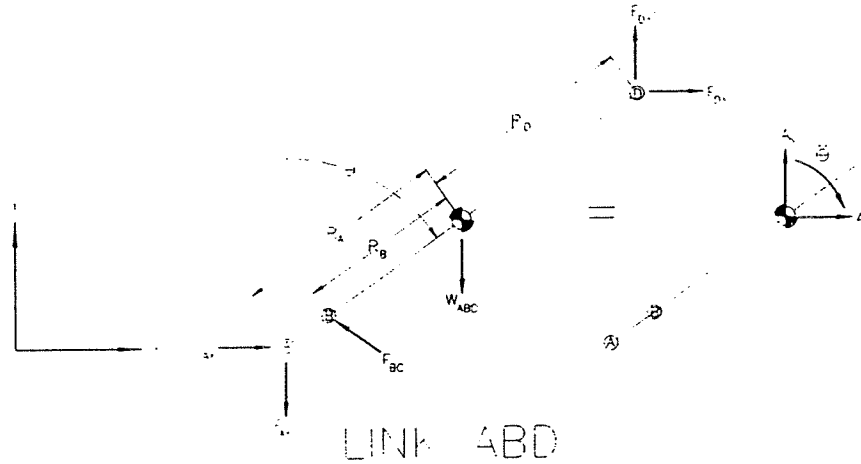
Figure A.3 *Link ABD Free Body Diagram*

FORCE AND MOMENT IN LINK ABD

$$\xrightarrow{+} \sum F_X = MA_X$$

$$F_{AX} - F_{BC}\sin(\Theta) + F_{DX} = M_{ABD}(A_{ABD})_X \tag{4}$$

$$+\uparrow \sum F_Y = MA_Y$$

$$-F_{AY} + F_{BC}\cos(\Theta) + F_{DY} = M_{ABD}(A_{ABD})_Y \tag{5}$$

$$\xrightarrow{+} \sum M_{CG} = I_{ABD}\ddot{\Theta}$$

$$-F_{AX}R_{AY} - F_{AY}R_{AX} + F_{BC}R_B\cos(2\Theta - 90) + F_{DX}R_{DY} - F_{DY}R_{DX} = I_{ABD}\ddot{\Theta} \tag{6}$$

STRESS IN LINK ABD Find the stress in link at joint B (tensile). Joint B has the max stress due to max bending moment and minimum cross sectional area.

$$M_B = \frac{F_{BC}\cos(2\Theta - 90)R_{AB}R_{BD}}{R_{LINK}} \quad \text{Where } R_{AB} = R_A - R_B \text{ and } R_{BD} = R_B + R_D \tag{7}$$

$$F_B = F_{DX}\sin(\Theta) + F_{DY}\cos(\Theta) \tag{8}$$

$$\sigma_B = \frac{M_B C}{I_{ABD}} + \frac{F_B}{A_{ABD}} \quad \text{Where } A_{ABD} \equiv \text{Cross sectional area of link ABD} \tag{9}$$

(without hole for joint)

APPENDIX A
FORCE, MOMENT, AND STRESS CALCULATIONS
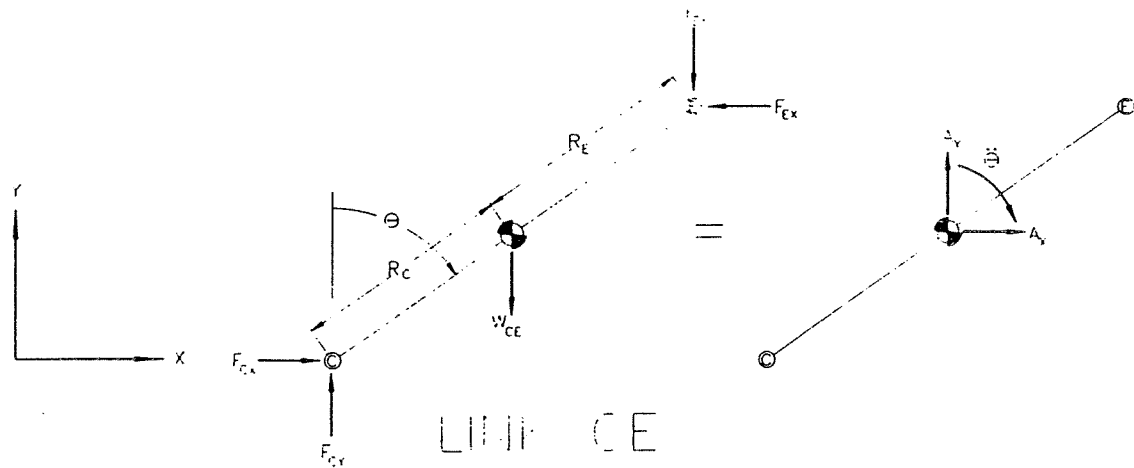
Figure A.4 *Link CE Free Body Diagram*

FORCE AN MOMENT IN LINK CE

$$\overset{+}{\rightarrow} \sum F_X = MA_X$$
$$F_{CX} - F_{EX} = M_{CD}(A_{CE})_X \tag{10}$$

$$+\uparrow \sum F_Y = MA_Y$$
$$F_{CY} - F_{EY} - W_{CE} = M_{CE}(A_{CE})_y \tag{11}$$

$$\overset{\rightarrow}{\underset{\leftarrow}{+}} \sum M_{CG} = I_{CE}\ddot{\Theta}$$
$$-F_{CX}R_{CY} + F_{CY}R_{CX} - F_{EX}R_{EY} + F_{EY}R_{EX} = I_{CE}\ddot{\Theta} \tag{12}$$

STRESS IN LINK CE (Compression)

Assume that F_{CE} is in line with link axis

$$\sigma_{CE} = \frac{F_{CE}}{A_{CE}} \qquad \text{Where } A_{CE} \equiv \text{ Cross sectional area of link CE} \tag{13}$$

Buckling for this link is evaluated near the end of this section.

APPENDIX A
FORCE, MOMENT, AND STRESS CALCULATIONS
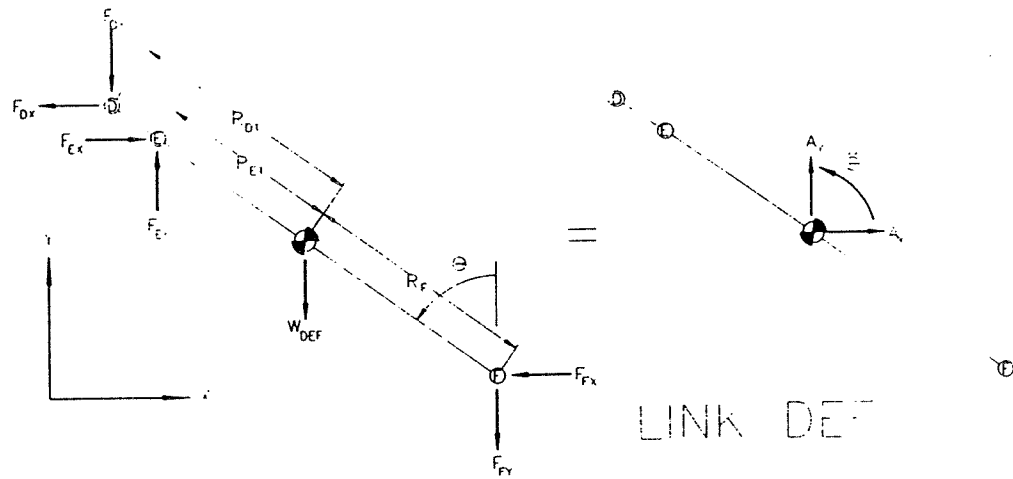
Figure A.5 *Link DEF Free Body Diagram*

FORCE AND MOMENT IN LINK DEF

$$\xrightarrow{+} \sum F_X = MA_X$$
$$-F_{DX} + F_{EX} - F_{FX} = M_{DEF}(A_{DEF})_X \tag{14}$$

$$+\uparrow \sum F_Y = MA_Y$$
$$-F_{DY} + F_{EY} - F_{FY} - W_{DEF} = M_{DEF}(A_{DEF})_Y \tag{15}$$

$$\overset{\leftarrow}{\underset{\rightarrow}{+}} \sum M_{CG} = I_{DEF}\ddot{\Theta}$$
$$F_{DX}R_{D1Y} + F_{DY}R_{D1X} - F_{EX}R_{E1Y} - F_{EY}R_{E1X} - M_{EEF}A_{EEF}R_{FY} - W_{EEF}R_{FX} = I_{DEF}\ddot{\Theta} \tag{16}$$

STRESS IN LINK DEF

Maximum stress occurs at joint E (tensile) due to max bending moment and force at minimum cross section.

$$M_E = R_{EF}(F_{EY}\sin(\Theta) + F_{EX}\cos(\Theta)) + R_{E1}W_{DEF}\sin(\Theta) \quad \text{Where } R_{EF} = R_{E1} + R_F \tag{17}$$

$$F_{E(TENSION)} = W_{DEF}\cos(\Theta) - F_{FX}\sin(\Theta) + F_{FY}\cos(\Theta) \tag{18}$$

$$\sigma_{E(TENSILE)} = \frac{M_E C_{CE}}{I_{CE}} + \frac{F_{E(TENSION)}}{A_{DEF}} \quad \text{Where } A_{DEF} \equiv \text{Cross sectional area of link DEF} \tag{19}$$
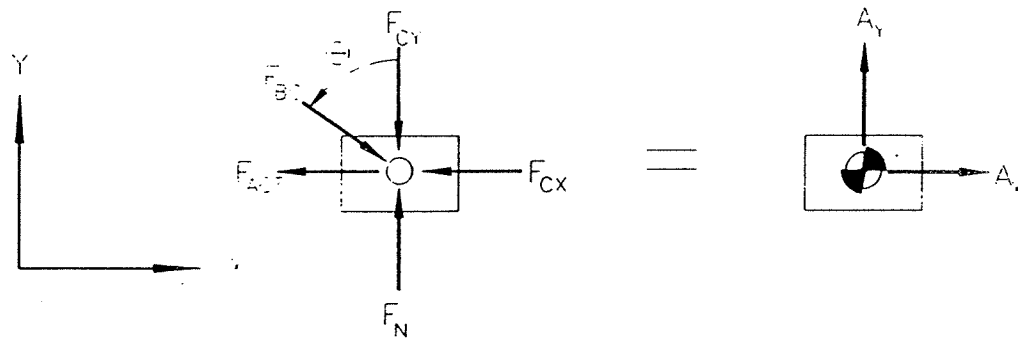
SLIDER, JOINT C

Figure A.6 *Slider, Joint C Free Body Diagram*

JOINT C SLIDER

Assume that the mass of the Slider is zero and no friction in the linear slide. Additionally, assume that the Slider is constrained to move in X direction only ($A_Y = 0$).

$$\sum F = MA = (0)A = 0$$
$$\Rightarrow \sum F = 0 \quad so,$$

$$\xrightarrow{\;} \sum F_X = 0$$
$$F_{BC}\sin(\Theta) - F_{CX} - F_{ACT} = 0 \tag{20}$$

$$+\uparrow \sum F_Y = 0$$
$$-F_{BC}\cos(\Theta) - F_{CY} + F_N = 0 \tag{21}$$

APPENDIX A
FORCE, MOMENT, AND STRESS CALCULATIONS
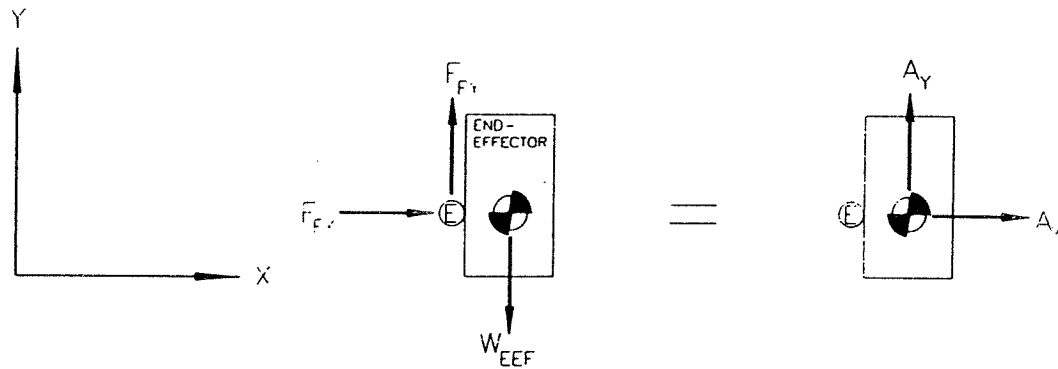
Figure A.7 *End-Effector Free Body Diagram*

END – EFFECTOR

Assume that the end - effector moves in X direction only due to the input (Slider) constrained to move in X direction.

$$\sum F_Y = M_{EEF}(A_{EEF})_Y = M_{EEF}(0) = 0$$
$$\Rightarrow \sum F_Y = 0$$

$$\xrightarrow{+} \sum F_X = M_{EEF}(A_{EEF})_X, \text{ but } (A_{EEF})_X = A_{EEF}$$
$$F_{FX} = M_{EEF} A_{EEF} \tag{22}$$

$$+\uparrow \sum F_Y = 0$$
$$F_{FY} - W_{EEF} = 0 \quad \Rightarrow \quad F_{FY} = W_{EEF} \tag{23}$$

APPENDIX A
FORCE, MOMENT, AND STRESS CALCULATIONS
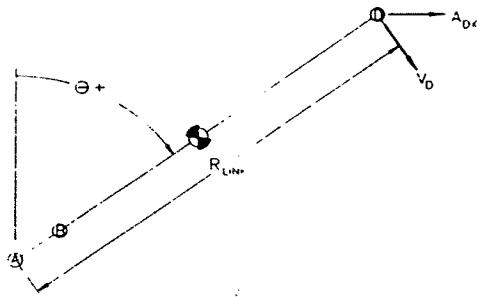
Determination of angular velocity

$$V_{DX} = \dot{\Theta} R_{LINK} \cos(\Theta) \quad and \quad V_{DX} = \frac{1}{2} V_{EEF}$$

$$\Rightarrow \quad V_{EEF} = 2\dot{\Theta} R_{LINK} \cos(\Theta)$$

$$or.. \quad \dot{\Theta} = \frac{V_{EEF}}{2 R_{LINK} \cos(\Theta)} \quad and \tag{24}$$

$$\dot{\Theta}^2 = \frac{V_{EEF}^2}{4 R_{LINK}^2 \cos^2(\Theta)}$$
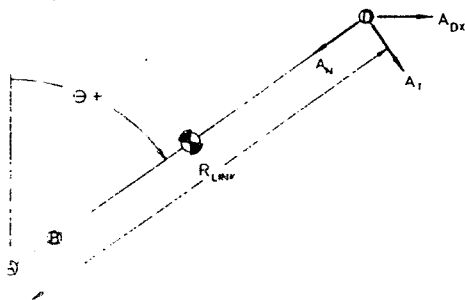
Determination of angular acceleration

$$A_{DX} = \ddot{\Theta} R_{LINK} \cos(\Theta) - \dot{\Theta}^2 R_{LINK} \sin(\Theta)$$

$$and \quad A_{DX} = \frac{1}{2} A_{EEF},$$

$$\Rightarrow \quad A_{EEF} = 2(\ddot{\Theta} R_{LINK} \cos(\Theta) - \dot{\Theta}^2 R_{LINK} \sin(\Theta)) \tag{25}$$

$$or.. \quad \ddot{\Theta} = \frac{A_{EEF}}{2 R_{LINK} \cos(\Theta)} + \frac{V_{EEF}^2 \tan(\Theta)}{4 R_{LINK}^2 \cos^2(\Theta)} \tag{26}$$
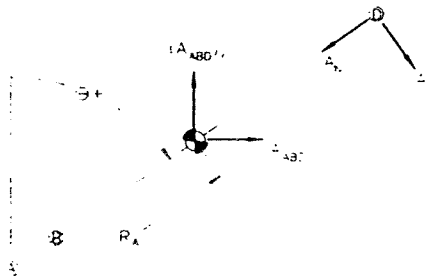
Determination of link ABD accelerations

$$A_{ABD})_X = \frac{1}{2} \frac{R_A}{R_{LINK}} A_{EEF} = 0.2367 A_{EEF} \tag{27}$$

$$(A_{ABD})_Y = -R_A (\ddot{\Theta} \sin(\Theta) + \dot{\Theta}^2 \cos(\Theta)) \tag{28}$$
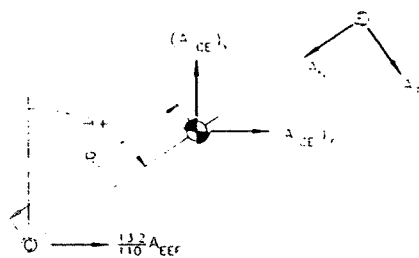
Determination of link CE accelerations

$$A_{CE})_X = \frac{13.2}{110} A_{EEF} + R_C (\ddot{\Theta} \cos(\Theta) - \dot{\Theta}^2 \sin(\Theta)) \tag{29}$$

$$(A_{CE})_Y = -R_C (\ddot{\Theta} \sin(\Theta) + \dot{\Theta}^2 \cos(\Theta)) \tag{30}$$
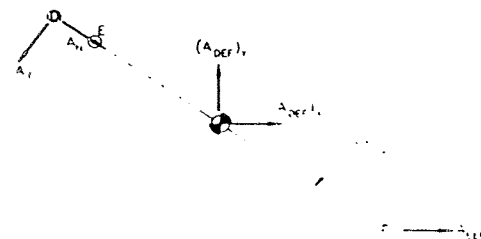
Determination of link DEF accelerations

$$(A_{DEF})_X = (\frac{R_{DI} + R_{LINK}}{2 R_{LINK}}) A_{EEF} = 0.737 A_{EEF} \tag{31}$$

$$(A_{DEF})_Y = -R_F (\ddot{\Theta} \sin(\Theta) + \dot{\Theta}^2 \cos(\Theta)) \tag{32}$$

Figure A.8 *Determination of Link Velocity and Accelerations*

APPENDIX A
FORCE, MOMENT, AND STRESS CALCULATIONS

The previous free body diagrams give us twelve equations and twelve unknowns. The values for link length, link weight, position, velocity and acceleration are known or specified. To determine the unknowns, solve individual equations for one unknown and substitute into other equations. This reduces equation (16) to one unknown, Force at E in the Y direction. Equation (33) shows the relation.

$$F_{EY} = \frac{B + 7.334(A)}{16.13\sin(\Theta)} \quad \text{Where} \tag{33}$$

$$A = \left[M_{EEF} A_{EEF} + M_{DEF}(A_{DEF})_X \right] R_{D1Y} + \left[W_{EEF} + W_{DEF} + M_{DEF}(A_{DEF})_Y \right] R_{D1X} + \tag{34}$$
$$M_{EEF} A_{EEF} R_{FY} + W_{EEF} R_{FX} + I_{DEF} \ddot{\Theta}$$

And

$$B = I_{CE} \ddot{\Theta} + M_{CE}(A_{CE})_X R_{CY} - \left[M_{CE}(A_{CE})_Y + W_{CE} \right] R_{CX} \tag{35}$$

Substituting the value for F_{EY} found with equation (33) into a simplified equation (16) yields the following equation.

$$F_{EX} = \frac{A}{1.1\cos(\Theta)} - F_{EY}\tan(\Theta) \tag{36}$$

Substituting F_{EX} and F_{EY} into equations (14) and (15) respectfully yields the following two equations.

$$F_{DX} = F_{EX} - M_{EEF} A_{EEF} - M_{DEF}(A_{DEF})_X \tag{37}$$
$$F_{DY} = F_{EY} - W_{EEF} - W_{DEF} - M_{DEF}(A_{DEF})_Y \tag{38}$$

Substituting F_{EX} and F_{EY} into equations (10) and (11) respectfully yields the following two equations.

$$F_{CX} = F_{EX} + M_{CE}(A_{CE})_X \tag{39}$$
$$F_{CY} = F_{EY} + M_{CE}(A_{CE})_Y + W_{CE} \tag{40}$$

APPENDIX A
FORCE, MOMENT, AND STRESS CALCULATIONS

To solve for F_{BC}, solve equations (4) and (5) for F_{AX} and F_{AY} respectfully and then substitute into equation (6) and solve the resultant equation for F_{BC}.

$$F_{BC} = \frac{C + \left[-F_{DX}\cos(\Theta) + F_{DY}\sin(\Theta)\right]R_D}{-2R_A\left[\cos(\Theta)\sin(\Theta)\right] + R_B\cos(2\Theta - 90)} \quad \text{Where} \tag{41}$$

$$C = I_{ABD}\ddot{\Theta} + R_A\left\{\left[M_{ABD}(A_{ABD})_X - F_{DX}\right]\cos(\Theta) + \left[-M_{ABD}(A_{ABD})_Y + F_{DY}\right]\sin(\Theta)\right\} \tag{42}$$

Substituting F_{BC} into equations (4) and (5) yields the following two equations which give the last two unknowns.

$$F_{AX} = M_{ABD}(A_{ABD})_X + F_{BC}\sin(\Theta) - F_{DX} \tag{43}$$

$$F_{AY} = M_{ABD}(A_{ABD})_Y + F_{BC}\cos(\Theta) + F_{DY} \tag{44}$$

APPENDIX A
FORCE, MOMENT, AND STRESS CALCULATIONS

RESULTS:

Critical Location	Stress	Arm Position	Arm Dynamics
Link ABD, Joint B	5157 psi	70° (extended)	Accel= -6 ft/sec/sec Vel=anything
Link BC	1173 psi	70° (extended)	Accel= -6ft/sec/sec Vel=anything
Link CD	864 psi	70° (extended)	Accel= +6 ft/sec/sec Vel=anything
Link DE, Joint E	2971 psi	70° (extended)	Accel= +6 ft/sec/sec Vel=anything

Table A.1 *Maximum Stresses in the Links*

The maximum stress in each critical location are shown in Table A.1 below.

APPENDIX A
FORCE, MOMENT, AND STRESS CALCULATIONS

DETERMINATION OF CRITICAL LOADING FOR LINK CE

Since link CE is in compression without any external loads or bending moments, buckling of the column is a concern that needs to be addressed. Determination of the critical loading is shown below. The calculations are taken from Mechanical Engineering Design [8]. It must be determined if the column is a short or a long column and use the appropriate equations to determine the critical load. The figure below shows the regions.
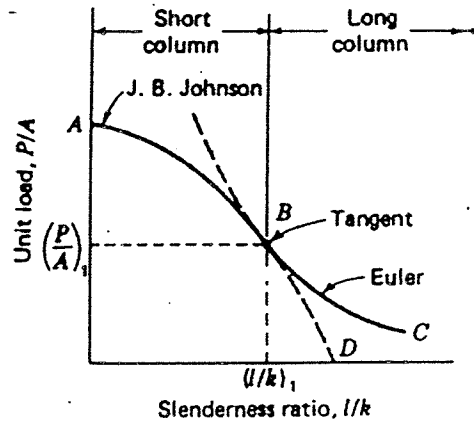
Figure A.9 *Determination of Column Loading Type*

J. B. Johnson formula:

$$\frac{P_{CR}}{A} = S_Y - \left(\frac{S_Y}{2\pi}\right)^2 \left(\frac{1}{CE}\right)\left(\frac{L}{k}\right)^2$$

Euler Formula:

$$\frac{P_{CR}}{A} = \frac{C\pi^2 E}{(L/k)^2}$$

(44) and (45)

Where:

P_{CR} = Critical Loading

A = Cross Sectional Area of Link CE

S_Y = Yield Strength

C = Distance from Neutral Axis to Outside of CE

E = Modulus of Elasticity

L = Length of the Column (Length of CE) = R_{CE}

k = Spring Constant of the Column = $\dfrac{AE}{L} = \dfrac{AE}{R_{CE}}$ (46)

Assume that the link is the static case so that transverse (small) load causing bending due to inertia loads can be ignored.

First we must determine $(L/k)_1$. From Mechanical Engineering Design

$$(L/k)_1 = \sqrt{\frac{2\pi^2 CE}{S_Y}} \tag{47}$$

$$= \sqrt{\frac{2\pi^2(1)(10x10^6)}{40x10^3}} = 70.2 \; in^2 \, / \, lb$$

Now calculate (L/k)

$$(L/k) = \frac{R_{CE}}{\left(\frac{AE}{R_{CE}}\right)} = \frac{R_{CE}^2}{AE} \tag{48}$$

$$= \frac{96.8^2}{(4^2 - 3.5^2)(10x10^6)} = 2.49x10^{-3} << 70.2 \; in^2 \, / \, lb$$

Since $(L/k) << (L/k)_1$, we must therefore use J. B. Johnson formula

$$\frac{P_{CR}}{A} = S_Y - \left(\frac{S_Y}{2\pi}\right)^2\left(\frac{1}{CE}\right)\left(\frac{L}{k}\right)^2$$

$$= S_Y - \left(\frac{S_Y}{2\pi}\right)\left(\frac{1}{(1)(10x10^6)}\right)(2.49x10^{-3})^2 = S_Y - S_Y(9.9x10^{-14})$$

$$\Rightarrow \frac{P_{CR}}{A} \cong S_Y \tag{49}$$

Use S_Y as the design stress with applicable factor of safety.

APPENDIX A
FORCE, MOMENT, AND STRESS CALCULATIONS

FORCE CALCULATIONS AT EACH JOINT

CONSTANTS:

	(feet)		(slugs)		(pounds)		(slugs*ft^2)
Ra=	4.34	Mabd=	6.24	Wabd=	201.26	Iabd=	78.64
Rb=	3.24	Mce=	2.37	Wce=	76.35	Ice=	20.41
Rc=	3.63	Mdef=	3.12	Wdef=	100.63	Idef=	39.32
Rd=	4.83	Meff=	6.21	Weff=	0.00		
Rd1=	4.34						
Re=	4.43	VARIABLE:		(ft/sec^2)		(ft/sec)	
Re1=	3.24		Aeff=	0.00	Veff=	0.00	
Rf=	4.83						
Rlink=	9.17						

THETA (deg)	Fex (pounds)	Fey (pounds)	Fdx (pounds)	Fdy (pounds)	Fcx (pounds)	Fcy (pounds)	Fbc (pounds)	Fax (pounds)	Fay (pounds)	Fact (pounds)	Fnormal (pounds)
15.00	57.78	181.33	57.78	80.70	57.78	257.68	581.38	92.70	642.27	92.70	819.25
20.00	78.48	181.33	78.48	80.70	78.48	257.68	597.80	125.98	642.45	125.98	819.43
25.00	100.55	181.33	100.55	80.70	100.55	257.68	619.95	161.46	642.57	161.46	819.55
30.00	124.49	181.33	124.49	80.70	124.49	257.68	648.89	199.96	642.66	199.96	819.64
35.00	150.98	181.33	150.98	80.70	150.98	257.68	686.11	242.56	642.73	242.56	819.71
40.00	180.93	181.33	180.93	80.70	180.93	257.68	733.76	290.72	642.79	290.72	819.77
45.00	215.62	181.33	215.62	80.70	215.62	257.68	795.00	346.53	642.85	346.53	819.83
50.00	256.97	181.33	256.97	80.70	256.97	257.68	874.64	413.05	642.91	413.05	819.89
55.00	307.94	181.33	307.94	80.70	307.94	257.68	980.29	495.07	642.98	495.07	819.96
60.00	373.47	181.33	373.47	80.70	373.47	257.68	1124.69	600.54	643.05	600.54	820.03
65.00	462.40	181.33	462.40	80.70	462.40	257.68	1330.83	743.74	643.14	743.74	820.12
70.00	592.41	181.33	592.41	80.70	592.41	257.68	1644.79	953.19	643.26	953.19	820.24

THETA (deg)	Mb (in lb)	Stress B (psi)	Stress BC (psi)	Stress CE (psi)	Me (in lb)	Stress E (psi)
15.00	3376.63	451.17	142.70	70.42	1012.37	155.32
20.00	4463.54	592.16	146.74	71.83	1337.81	196.22
25.00	5516.56	729.49	152.17	73.76	1653.07	235.62
30.00	6527.67	862.20	159.28	76.31	1955.74	273.23
35.00	7489.19	989.44	168.41	79.64	2243.54	308.76
40.00	8393.83	1110.42	180.11	83.96	2514.26	341.94
45.00	9234.72	1224.52	195.14	89.60	2765.84	372.51
50.00	10005.49	1331.29	214.69	97.04	2996.37	400.25
55.00	10700.35	1430.60	240.62	107.07	3204.10	424.95
60.00	11314.09	1522.78	276.06	121.00	3387.45	446.41
65.00	11842.21	1609.11	326.66	141.16	3545.01	464.47
70.00	12281.03	1692.80	403.73	172.27	3675.60	479.00
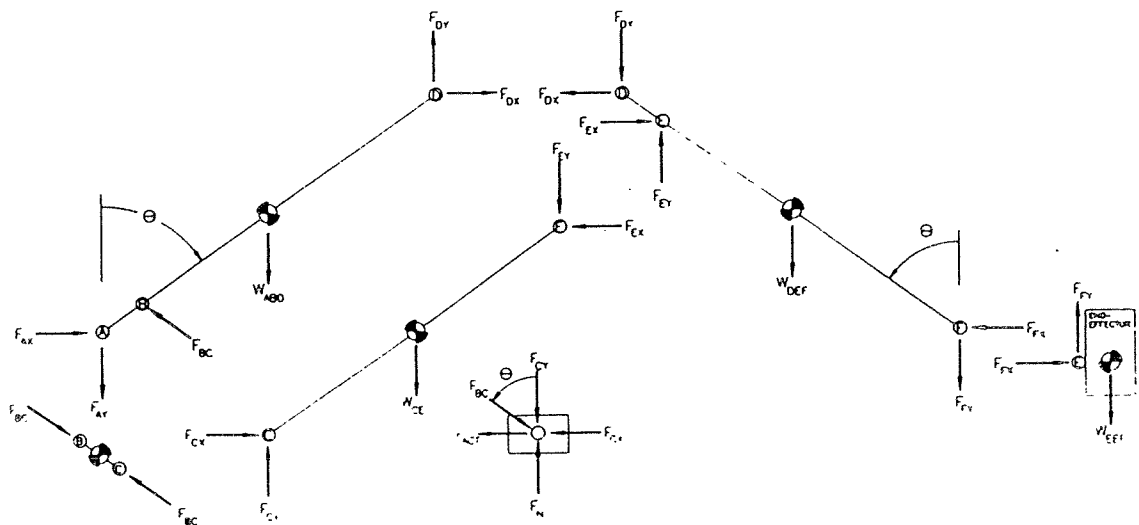
Table A.2 *Link Forces and Stresses with Weef=0, Velocity=0, and Acceleration=0*

APPENDIX A
FORCE, MOMENT, AND STRESS CALCULATIONS

FORCE CALCULATIONS AT EACH JOINT
CONSTANTS:

	(feet)		(slugs)		(pounds)		(slugs*ft^2)
Ra=	4.34	Mabd=	6.24	Wabd=	201.26	Iabd=	78.64
Rb=	3.24	Mce=	2.37	Wce=	76.35	Ice=	20.41
Rc=	3.63	Mdef=	3.12	Wdef=	100.63	Idef=	39.32
Rd=	4.83	Meff=	6.21	Weff=	200.00		
Rd1=	4.34						
Re=	4.43		VARIABLE:		(ft/sec^2)		(ft/sec)
Re1=	3.24			Aeff=	0.00	Veff=	0.00
Rf=	4.83						
Rlink=	9.17						

THETA (deg)	Fex (pounds)	Fey (pounds)	Fdx (pounds)	Fdy (pounds)	Fcx (pounds)	Fcy (pounds)	Fbc (pounds)	Fax (pounds)	Fay (pounds)	Fact (pounds)	Fnormal (pounds)
15.00	281.00	1014.92	281.00	714.29	281.00	1091.27	1441.07	91.98	2106.26	91.98	2483.24
20.00	381.70	1014.92	381.70	714.29	381.70	1091.27	1481.78	125.10	2106.71	125.10	2483.69
25.00	489.02	1014.92	489.02	714.29	489.02	1091.27	1536.69	160.41	2107.00	160.41	2483.98
30.00	605.47	1014.92	605.47	714.29	605.47	1091.27	1608.42	198.74	2107.22	198.74	2484.20
35.00	734.31	1014.92	734.31	714.29	734.31	1091.27	1700.68	241.16	2107.40	241.16	2484.38
40.00	879.97	1014.92	879.97	714.29	879.97	1091.27	1818.78	289.12	2107.55	289.12	2484.53
45.00	1048.71	1014.92	1048.71	714.29	1048.71	1091.27	1970.59	344.71	2107.70	344.71	2484.68
50.00	1249.80	1014.92	1249.80	714.29	1249.80	1091.27	2168.00	410.99	2107.85	410.99	2484.83
55.00	1497.71	1014.92	1497.71	714.29	1497.71	1091.27	2429.88	492.73	2108.01	492.73	2484.99
60.00	1816.41	1014.92	1816.41	714.29	1816.41	1091.27	2787.80	597.89	2108.18	597.89	2485.16
65.00	2248.96	1014.92	2248.96	714.29	2248.96	1091.27	3298.76	740.74	2108.40	740.74	2485.38
70.00	2881.30	1014.92	2881.30	714.29	2881.30	1091.27	4076.99	949.82	2108.70	949.82	2485.68

THETA (deg)	Mb (in lb)	Stress B (psi)	Stress BC (psi)	Stress CE (psi)	Me (in lb)	Stress E (psi)
15.00	8369.76	1230.41	353.72	300.50	6023.10	847.33
20.00	11063.92	1583.01	363.72	308.29	7959.32	1092.72
25.00	13674.05	1927.65	377.19	318.89	9834.96	1329.79
30.00	16180.32	2262.18	394.80	332.79	11635.74	1556.74
35.00	18563.68	2584.71	417.45	350.75	13347.98	1771.84
40.00	20806.02	2893.76	446.44	373.83	14958.62	1973.46
45.00	22890.35	3188.36	483.70	403.60	16455.43	2160.07
50.00	24800.90	3468.34	532.16	442.45	17826.99	2330.23
55.00	26523.26	3734.81	596.44	494.16	19062.89	2482.65
60.00	28044.55	3991.09	684.29	565.07	20153.70	2616.19
65.00	29353.63	4244.72	809.71	666.60	21091.13	2729.81
70.00	30441.35	4512.53	1000.73	821.61	21868.05	2822.65
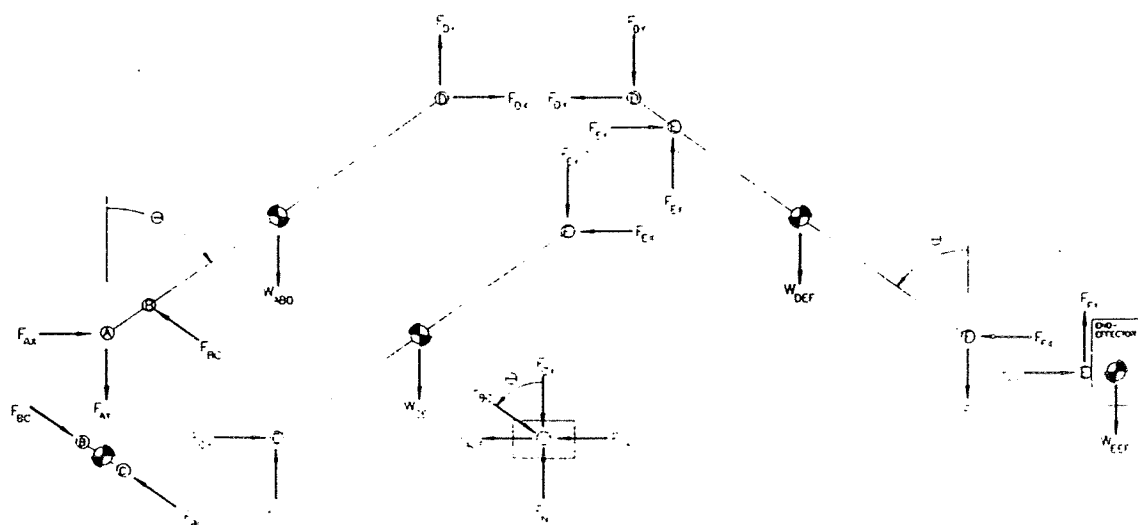
Table A.3 *Link Forces and Stresses with Weef=200, Velocity=0, and Acceleration=0*

APPENDIX A
FORCE, MOMENT, AND STRESS CALCULATIONS

FORCE CALCULATIONS AT EACH JOINT
CONSTANTS:

	(feet)		(slugs)		(pounds)		(slugs*ft^2)
Ra=	4.34	Mabd=	6.24	Wabd=	201.26	Iabd=	78.64
Rb=	3.24	Mce=	2.37	Wce=	76.35	Ice=	20.41
Rc=	3.63	Mdef=	3.12	Wdef=	100.63	Idef=	39.32
Rd=	4.83	Meff=	6.21	Weff=	200.00		
Rd1=	4.34						
Re=	4.43		VARIABLE:	(ft/sec^2)		(ft/sec)	
Re1=	3.24			Aeff=	6.00	Veff=	0.00
Rf=	4.83						
Rlink=	9.17						

THETA (deg)	Fex (pounds)	Fey (pounds)	Fdx (pounds)	Fdy (pounds)	Fcx (pounds)	Fcy (pounds)	Fbc (pounds)	Fax (pounds)	Fay (pounds)	Fact (pounds)	Fnormal (pounds)
15.00	467.46	1722.46	416.41	1423.15	471.98	1798.06	443.34	-292.80	1853.76	-357.24	2226.29
20.00	567.86	1535.33	516.80	1236.49	572.38	1610.65	716.16	-263.00	1912.69	-327.44	2283.62
25.00	674.76	1420.60	623.71	1122.27	679.28	1495.64	905.20	-232.29	1946.80	-296.73	2316.03
30.00	790.64	1342.01	739.59	1044.23	795.17	1416.73	1061.04	-200.21	1968.23	-264.65	2335.62
35.00	918.71	1283.99	867.66	986.81	923.23	1358.36	1207.46	-166.23	1982.10	-230.67	2347.45
40.00	1063.31	1238.73	1012.26	942.23	1067.84	1312.71	1359.18	-129.74	1990.86	-194.17	2353.91
45.00	1230.59	1201.88	1179.54	906.18	1235.12	1275.41	1528.29	-90.02	1995.70	-154.46	2356.07
50.00	1429.62	1170.80	1378.57	876.05	1434.14	1243.79	1727.62	-46.28	1997.10	-110.71	2354.28
55.00	1674.48	1143.77	1623.43	850.18	1679.01	1216.10	1973.80	2.27	1994.96	-62.16	2348.22
60.00	1988.46	1119.60	1937.41	827.98	1992.98	1191.07	2291.51	55.96	1988.61	-8.48	2336.82
65.00	2413.14	1097.36	2362.08	807.30	2417.66	1167.66	2721.29	113.11	1976.37	48.67	2317.73
70.00	3030.96	1076.23	2979.91	789.15	3035.48	1144.84	3336.31	164.06	1954.58	99.63	2285.92

| THETA (deg)	Mb (in lb)	Stress B (psi)	Stress BC (psi)	Stress CE (psi)	Me (in lb)	Stress E (psi)
15.00	2574.92	641.22	108.82	495.73	9506.97	1290.07
20.00	5347.27	965.33	175.79	455.82	11348.57	1522.54
25.00	8054.82	1299.21	222.19	438.05	13103.80	1743.42
30.00	10673.77	1632.59	260.44	433.23	14759.30	1951.03
35.00	13179.95	1959.65	296.38	437.98	16302.47	2143.80
40.00	15548.40	2276.38	333.62	451.25	17721.57	2320.25
45.00	17752.60	2579.68	375.13	473.45	19005.80	2479.03
50.00	19763.12	2867.05	424.06	506.23	20145.38	2618.96
55.00	21544.94	3136.56	484.49	552.84	21131.64	2738.95
60.00	23052.01	3386.91	562.47	619.14	21957.08	2838.09
65.00	24215.06	3617.75	667.97	715.96	22615.42	2915.64
70.00	24910.98	3830.53	818.93	865.12	23101.63	2971.00
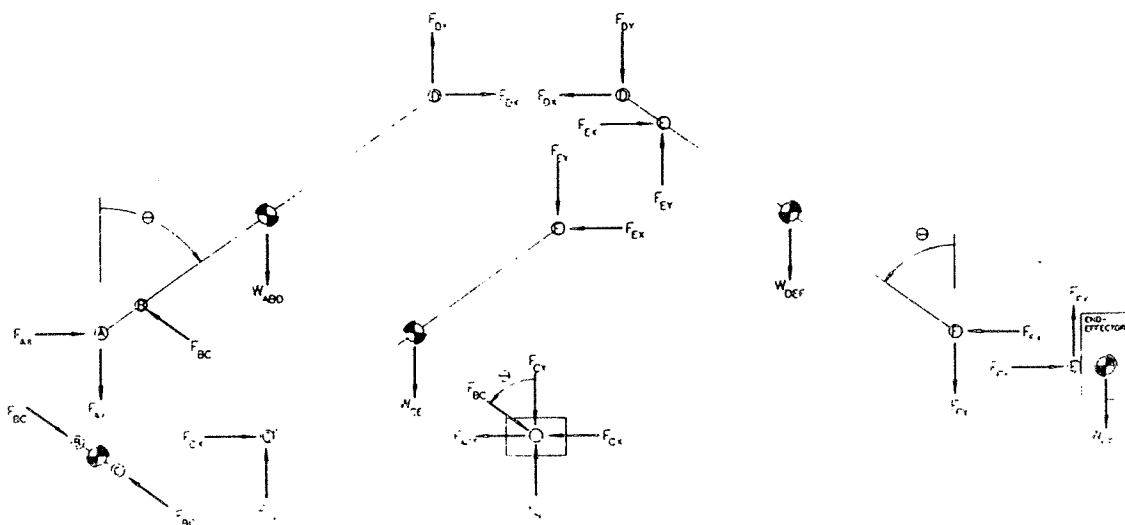
Table A.4 *Link Forces and Stresses with Weef=200, Velocity=0, and Acceleration=6*

APPENDIX A
FORCE, MOMENT, AND STRESS CALCULATIONS

FORCE CALCULATIONS AT EACH JOINT

CONSTANTS:

	(feet)		(slugs)		(pounds)		(slugs*ft^2)
Ra=	4.34	Mabd=	6.24	Wabd=	201.26	Iabd=	78.64
Rb=	3.24	Mce=	2.37	Wce=	76.35	Ice=	20.41
Rc=	3.63	Mdef=	3.12	Wdef=	100.63	Idef=	39.32
Rd=	4.83	Meff=	6.21	Weff=	200.00		
Rd1=	4.34						
Re=	4.43	VARIABLE:		(ft/sec^2)		(ft/sec)	
Re1=	3.24			Aeff=	6.00	Veff=	1.00
Rf=	4.83						
Rlink=	9.17						

THETA (deg)	Fex (pounds)	Fey (pounds)	Fdx (pounds)	Fdy (pounds)	Fcx (pounds)	Fcy (pounds)	Fbc (pounds)	Fax (pounds)	Fay (pounds)	Fact (pounds)	Fnormal (pounds)
15.00	467.44	1722.43	416.39	1423.18	471.97	1798.00	442.73	-292.94	1853.28	-357.38	2225.65
20.00	567.84	1535.30	516.79	1236.52	572.36	1610.59	715.48	-263.22	1912.17	-327.65	2282.92
25.00	674.73	1420.57	623.68	1122.30	679.26	1495.57	904.41	-232.60	1946.22	-297.03	2315.25
30.00	790.60	1341.97	739.55	1044.26	795.13	1416.65	1060.09	-200.64	1967.56	-265.08	2334.72
35.00	918.65	1283.94	867.60	986.84	923.18	1358.27	1206.28	-166.85	1981.32	-231.29	2346.39
40.00	1063.23	1238.67	1012.18	942.28	1067.76	1312.60	1357.64	-130.64	1989.90	-195.08	2352.61
45.00	1230.47	1201.81	1179.42	906.23	1234.99	1275.27	1526.16	-91.39	1994.48	-155.83	2354.43
50.00	1429.42	1170.70	1378.37	876.12	1433.94	1243.60	1724.50	-48.46	1995.47	-112.90	2352.09
55.00	1674.14	1143.64	1623.09	850.28	1678.67	1215.83	1968.89	-1.41	1992.67	-65.85	2345.13
60.00	1987.84	1119.39	1936.79	827.66	1992.36	1190.66	2283.00	49.21	1985.15	-15.22	2332.16
65.00	2411.86	1097.02	2360.81	807.55	2416.39	1166.98	2704.63	99.27	1970.65	34.83	2310.01
70.00	3027.89	1075.59	2976.83	789.62	3032.41	1143.55	3297.45	130.62	1943.78	66.18	2271.35

| THETA (deg)	Mb (in lb)	Stress B (psi)	Stress BC (psi)	Stress CE (psi)	Me (in lb)	Stress E (psi)
15.00	2571.38	640.78	108.67	495.71	9506.97	1290.07
20.00	5342.18	964.68	175.62	455.81	11348.57	1522.54
25.00	8047.82	1298.32	222.00	438.03	13103.80	1743.42
30.00	10664.27	1631.37	260.21	433.21	14759.30	1951.03
35.00	13167.07	1958.00	296.09	437.95	16302.47	2143.80
40.00	15530.75	2274.12	333.24	451.21	17721.57	2320.25
45.00	17727.91	2576.51	374.61	473.40	19005.80	2479.03
50.00	19727.51	2862.48	423.30	506.16	20145.38	2618.96
55.00	21491.34	3129.66	483.28	552.72	21131.64	2738.95
60.00	22966.45	3375.87	560.38	618.94	21957.08	2838.09
65.00	24066.77	3598.58	663.87	715.58	22615.42	2915.64
70.00	24620.84	3792.87	809.39	864.23	23101.63	2971.00

Table A.5 *Link Forces and Stresses with Weef=200, Velocity=1, and Acceleration=6*

APPENDIX A
FORCE, MOMENT, AND STRESS CALCULATIONS

FORCE CALCULATIONS AT EACH JOINT
CONSTANTS:

	(feet)		(slugs)		(pounds)		(slugs*ft^2)
Ra=	4.34	Mabd=	6.24	Wabd=	201.26	Iabd=	78.64
Rb=	3.24	Mce=	2.37	Wce=	76.35	Ice=	20.41
Rc=	3.63	Mdef=	3.12	Wdef=	100.63	Idef=	39.32
Rd=	4.83	Meff=	6.21	Weff=	200.00		
Rd1=	4.34						
Re=	4.43	VARIABLE:		(ft/sec^2)		(ft/sec)	
Re1=	3.24		Aeff=	-6.00	Veff=	1.00	
Rf=	4.83						
Rlink=	9.17						

THETA (deg)	Fex (pounds)	Fey (pounds)	Fdx (pounds)	Fdy (pounds)	Fcx (pounds)	Fcy (pounds)	Fbc (pounds)	Fax (pounds)	Fay (pounds)	Fact (pounds)	Fnormal (pounds)
15.00	94.53	307.34	145.58	5.44	90.00	384.42	2438.20	476.61	2358.27	541.05	2739.53
20.00	195.52	494.47	246.57	192.10	190.99	571.82	2246.73	512.99	2300.21	577.43	2683.05
25.00	303.25	609.19	354.30	306.33	298.73	686.82	2167.39	552.82	2266.63	617.25	2651.15
30.00	420.26	687.78	471.31	384.37	415.74	765.72	2154.86	597.26	2245.55	661.70	2631.89
35.00	549.86	745.80	600.91	441.80	545.33	824.08	2192.72	647.92	2231.91	712.36	2620.24
40.00	696.54	791.05	747.59	486.38	692.01	869.70	2276.84	707.07	2223.29	771.51	2613.87
45.00	866.69	827.88	917.74	522.45	862.06	906.97	2410.76	778.06	2218.48	842.50	2611.64
50.00	1069.78	858.93	1120.83	552.60	1065.25	938.55	2605.27	866.06	2216.98	930.50	2613.18
55.00	1320.60	885.92	1371.65	578.49	1316.07	966.16	2881.05	979.51	2218.76	1043.95	2618.66
60.00	1643.74	910.03	1694.80	601.22	1639.22	991.06	3275.58	1133.08	2224.31	1197.52	2628.85
65.00	2083.51	932.13	2134.56	621.53	2078.98	1014.19	3859.57	1354.54	2234.72	1418.98	2645.31
70.00	2728.56	952.96	2779.61	639.90	2724.04	1036.41	4778.81	1702.14	2252.02	1766.58	2670.86

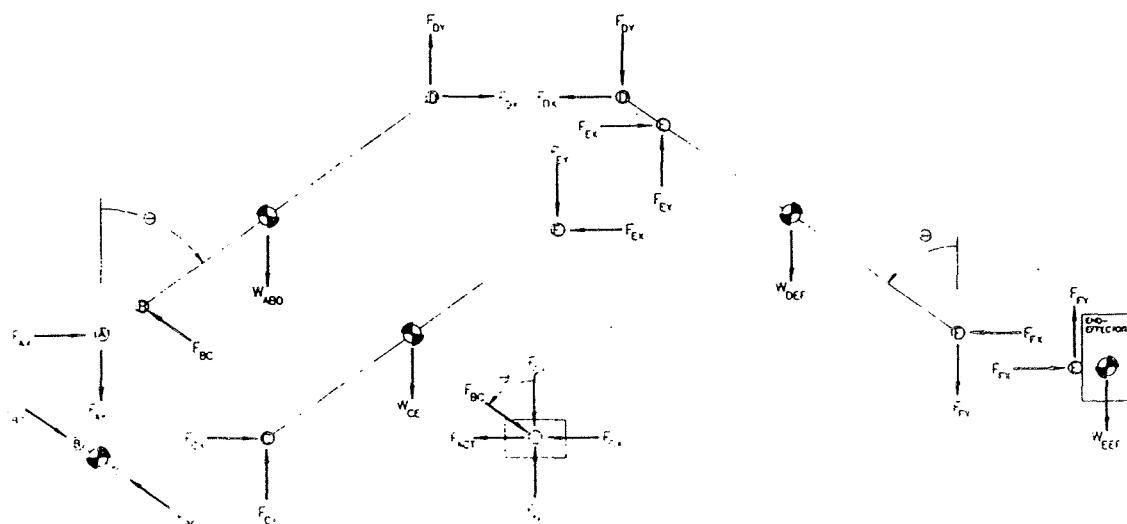| THETA (deg)	Mb (in lb)	Stress B (psi)	Stress BC (psi)	Stress CE (psi)	Me (in lb)	Stress E (psi)
15.00	14161.05	1819.14	598.48	105.28	2539.23	404.58
20.00	16775.48	2200.05	551.48	160.77	4570.06	662.89
25.00	19286.28	2555.20	532.01	199.73	6566.11	916.15
30.00	21677.38	2890.55	528.93	232.35	8512.19	1162.45
35.00	23934.53	3208.13	538.22	263.51	10393.49	1399.89
40.00	26046.00	3508.88	558.87	296.38	12195.68	1626.68
45.00	28003.42	3793.87	591.74	333.70	13905.06	1841.10
50.00	29803.07	4065.05	639.49	378.59	15508.61	2041.50
55.00	31447.98	4326.17	707.18	435.37	16994.13	2226.36
60.00	32951.55	4584.24	804.02	510.81	18350.32	2394.28
65.00	34343.91	4852.51	947.37	616.84	19566.84	2543.97
70.00	35681.57	5156.88	1173.00	777.21	20634.46	2674.31

Table A.6 *Link Forces and Stresses with Weef=200, Velocity=1, and Acceleration=-6*

APPENDIX A
FORCE, MOMENT, AND STRESS CALCULATIONS

FORCE CALCULATIONS AT EACH JOINT
CONSTANTS:

	(feet)		(slugs)		(pounds)		(slugs*ft^2)
Ra=	4.34	Mabd=	6.24	Wabd=	201.26	Iabd=	78.64
Rb=	3.24	Mce=	2.37	Wce=	76.35	Ice=	20.41
Rc=	3.63	Mdef=	3.12	Wdef=	100.63	Idef=	39.32
Rd=	4.83	Meff=	6.21	Weff=	200.00		
Rd1=	4.34						
Re=	4.43	VARIABLE:		(ft/sec^2)		(ft/sec)	
Re1=	3.24			Aeff=	6.00	Veff=	-1.00
Rf=	4.83						
Rlink=	9.17						

THETA (deg)	Fex (pounds)	Fey (pounds)	Fdx (pounds)	Fdy (pounds)	Fcx (pounds)	Fcy (pounds)	Fbc (pounds)	Fax (pounds)	Fay (pounds)	Fact (pounds)	Fnormal (pounds)
15.00	467.44	1722.43	416.39	1423.18	471.97	1798.00	442.73	-292.94	1853.28	-357.38	2225.65
20.00	567.84	1535.30	516.79	1236.52	572.36	1610.59	715.48	-263.22	1912.17	-327.65	2282.92
25.00	674.73	1420.57	623.68	1122.30	679.26	1495.57	904.41	-232.60	1946.22	-297.03	2315.25
30.00	790.60	1341.97	739.55	1044.26	795.13	1416.65	1060.09	-200.64	1967.56	-265.08	2334.72
35.00	918.65	1283.94	867.60	986.84	923.18	1358.27	1206.28	-166.85	1981.32	-231.29	2346.39
40.00	1063.23	1238.67	1012.18	942.28	1067.76	1312.60	1357.64	-130.64	1989.90	-195.08	2352.61
45.00	1230.47	1201.81	1179.42	906.23	1234.99	1275.27	1526.16	-91.39	1994.48	-155.83	2354.43
50.00	1429.42	1170.70	1378.37	876.12	1433.94	1243.60	1724.50	-48.46	1995.47	-112.90	2352.09
55.00	1674.14	1143.64	1623.09	850.28	1678.67	1215.83	1968.89	-1.41	1992.67	-65.85	2345.13
60.00	1987.84	1119.39	1936.79	827.66	1992.36	1190.66	2283.00	49.21	1985.15	-15.22	2332.16
65.00	2411.86	1097.02	2360.81	807.55	2416.39	1166.98	2704.63	99.27	1970.65	34.83	2310.01
70.00	3027.89	1075.59	2976.83	789.62	3032.41	1143.55	3297.45	130.62	1943.78	66.18	2271.35

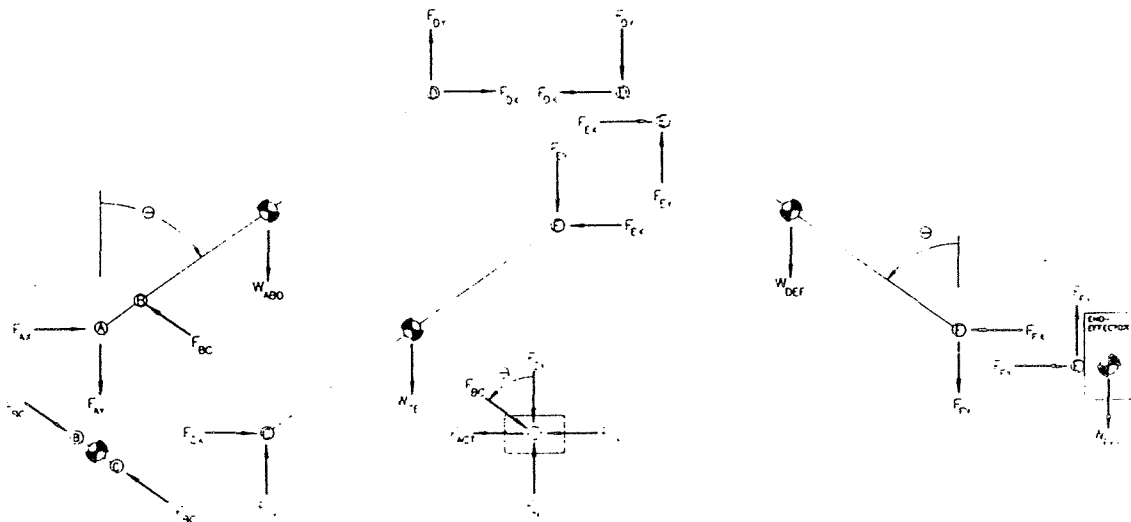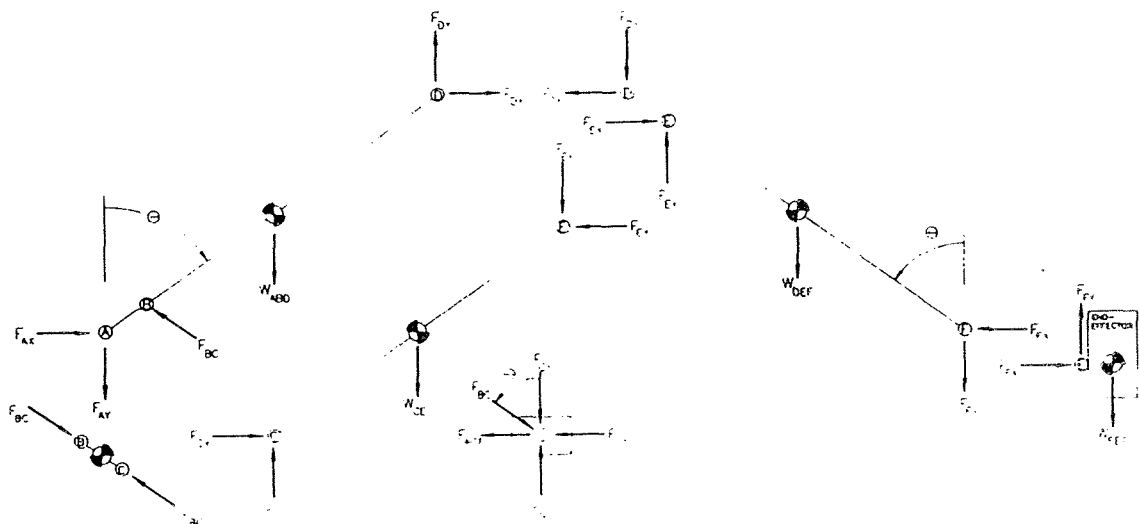| THETA (deg)	Mb (in lb)	Stress B (psi)	Stress BC (psi)	Stress CE (psi)	Me (in lb)	Stress E (psi)
15.00	2571.38	640.78	108.67	495.71	9506.97	1290.07
20.00	5342.18	964.68	175.62	455.81	11348.57	1522.54
25.00	8047.82	1298.32	222.00	438.03	13103.80	1743.42
30.00	10664.27	1631.37	260.21	433.21	14759.30	1951.03
35.00	13167.07	1958.00	296.09	437.95	16302.47	2143.80
40.00	15530.75	2274.12	333.24	451.21	17721.57	2320.25
45.00	17727.91	2576.51	374.61	473.40	19005.80	2479.03
50.00	19727.51	2862.48	423.30	506.16	20145.38	2618.96
55.00	21491.34	3129.66	483.28	552.72	21131.64	2738.95
60.00	22966.45	3375.87	560.38	618.94	21957.08	2838.09
65.00	24066.77	3598.58	663.87	715.58	22615.42	2915.64
70.00	24620.84	3792.87	809.39	864.23	23101.63	2971.00

Table A.7 *Link Forces and Stresses with Weef=200, Velocity=-1, and Acceleration=6*

APPENDIX A
FORCE, MOMENT, AND STRESS CALCULATIONS

FORCE CALCULATIONS AT EACH JOINT

CONSTANTS:

	(feet)		(slugs)		(pounds)		(slugs*ft^2)
Ra=	4.34	Mabd=	6.24	Wabd=	201.26	Iabd=	78.64
Rb=	3.24	Mce=	2.37	Wce=	76.35	Ice=	20.41
Rc=	3.63	Mdef=	3.12	Wdef=	100.63	Idef=	39.32
Rd=	4.83	Meff=	6.21	Weff=	200.00		
Rd1=	4.34						
Re=	4.43	VARIABLE:		(ft/sec^2)			(ft/sec)
Re1=	3.24		Aeff=	-6.00	Veff=	-1.00	
Rf=	4.83						
Rlink=	9.17						

THETA (deg)	Fex (pounds)	Fey (pounds)	Fdx (pounds)	Fdy (pounds)	Fcx (pounds)	Fcy (pounds)	Fbc (pounds)	Fax (pounds)	Fay (pounds)	Fact (pounds)	Fnormal (pounds)
15.00	94.53	307.34	145.58	5.44	90.00	384.42	2438.20	476.61	2358.27	541.05	2739.53
20.00	195.52	494.47	246.57	192.10	190.99	571.82	2246.73	512.99	2300.21	577.43	2683.05
25.00	303.25	609.19	354.30	306.33	298.73	686.82	2167.39	552.82	2266.63	617.25	2651.15
30.00	420.26	687.78	471.31	384.37	415.74	765.72	2154.86	597.26	2245.55	661.70	2631.89
35.00	549.86	745.80	600.91	441.80	545.33	824.08	2192.72	647.92	2231.91	712.36	2620.24
40.00	696.54	791.05	747.59	486.38	692.01	869.70	2276.84	707.07	2223.29	771.51	2613.87
45.00	866.69	827.88	917.74	522.45	862.16	906.97	2410.76	778.06	2218.48	842.50	2611.64
50.00	1069.78	858.93	1120.83	552.60	1065.25	938.55	2605.27	866.06	2216.98	930.50	2613.18
55.00	1320.60	885.92	1371.65	578.49	1316.07	966.16	2881.05	979.51	2218.76	1043.95	2618.66
60.00	1643.74	910.03	1694.80	601.22	1639.22	991.06	3275.58	1133.08	2224.31	1197.52	2628.85
65.00	2083.51	932.13	2134.56	621.53	2078.98	1014.19	3859.57	1354.54	2234.72	1418.98	2645.31
70.00	2728.56	952.96	2779.61	639.90	2724.04	1036.41	4778.81	1702.14	2252.02	1766.58	2670.86

THETA (deg)	Mb (in lb)	Stress B (psi)	Stress BC (psi)	Stress CE (psi)	Me (in lb)	Stress E (psi)
15.00	14161.05	1819.14	598.48	105.28	2539.23	404.58
20.00	16775.48	2200.05	551.48	160.77	4570.06	662.89
25.00	19286.28	2555.20	532.01	199.73	6566.11	916.15
30.00	21677.38	2890.55	528.93	232.35	8512.19	1162.45
35.00	23934.53	3208.13	538.22	263.51	10393.49	1399.89
40.00	26046.00	3508.88	558.87	296.38	12195.68	1626.68
45.00	28003.42	3793.87	591.74	333.70	13905.06	1841.10
50.00	29803.07	4065.05	639.49	378.59	15508.61	2041.50
55.00	31447.98	4326.17	707.18	435.37	16994.13	2226.36
60.00	32951.55	4584.24	804.02	510.81	18350.32	2394.28
65.00	34343.91	4852.51	947.37	616.84	19566.84	2543.97
70.00	35681.57	5156.88	1173.00	777.21	20634.46	2674.31

Table A.8 *Link Forces and Stresses with Weef=200, Velocity=-1, and Acceleration=-6*

APPENDIX B
DETAILED DRAWINGS

APPENDIX B
DETAILED DRAWINGS

SECTION A-A

APPENDIX B
DETAILED DRAWINGS

APPENDIX B
DETAILED DRAWINGS

SHAFT, JOINT

NOTES: UNLESS OTHERWISE SPECIFIED
1) ALL DIMENSIONS IN INCHES
2) BREAK ALL SHARP EDGES

PILLOW BLOCK JOINT

NOTES: UNLESS OTHERWISE SPECIFIED
1) BREAK ALL SHARP EDGES
2) ALL DIMENSIONS IN INCHES
3) SURFACE   FLAT BLACK ENAMEL WITH
APPROPRIATE PRIMER WITH EXCEPTION
OF ALL HOLES AND THREADS

APPENDIX B
DETAILED DRAWINGS

X8 Ø0.41
CBORE FOR 3/8-16 UNC
SOCKET HEAD CAP SCREW

Ø0.43

X4 5/16-18 UNC

NOTES: UNLESS OTHERWISE SPECIFIED
1) BREAK ALL SHARP EDGES
2) ALL DIMENSIONS IN INCHES
3) PART IS SYMMETRICAL ABOUT THE
   LONG AXIS
4) SURFACE: FLAT BLACK ENAMEL WITH
   APPROPRIATE PRIMER WITH EXCEPTION
   OFF ALL THREADS

AHMCT CENTER
UNIVERSITY OF CALIFORNIA, DAVIS

PLATE, JOINT

7.48

$1.502 {}^{+0.000}_{-0.001}$

X2 5/8-11 UNC
1.00 DEEP

63

NOTES: UNLESS OTHERWISE SPECIFIED
1) BREAK ALL SHARP EDGES
2) ALL DIMENSIONS IN INCHES

AHMCT CENTER
UNIVERSITY OF CALIFORNIA, DAVIS

SHAFT, JOINT

APPENDIX B
DETAILED DRAWINGS

APPENDIX B
DETAILED DRAWINGS

APPENDIX B
DETAILED DRAWINGS

NOTES: UNLESS OTHERWISE SPECIFIED
1) ALL DIMENSIONS IN INCHES
2) BREAK ALL SHARP EDGES

SHAFT JOINT A

X4 Ø0.28 THRU

0.25

3X Ø0.22 THRU EQUALLY
SPACED ON A Ø1.875 B.C

ENCODER ADAPTER

M1063

APPENDIX B
DETAILED DRAWINGS

APPENDIX B
DETAILED DRAWINGS

APPENDIX B
DETAILED DRAWINGS

APPENDIX B
DETAILED DRAWINGS

13.99
12.993
12.000
10.993
5.000
2.000
1.000
1.000

X4 R0.25

6.720
7.720

△1

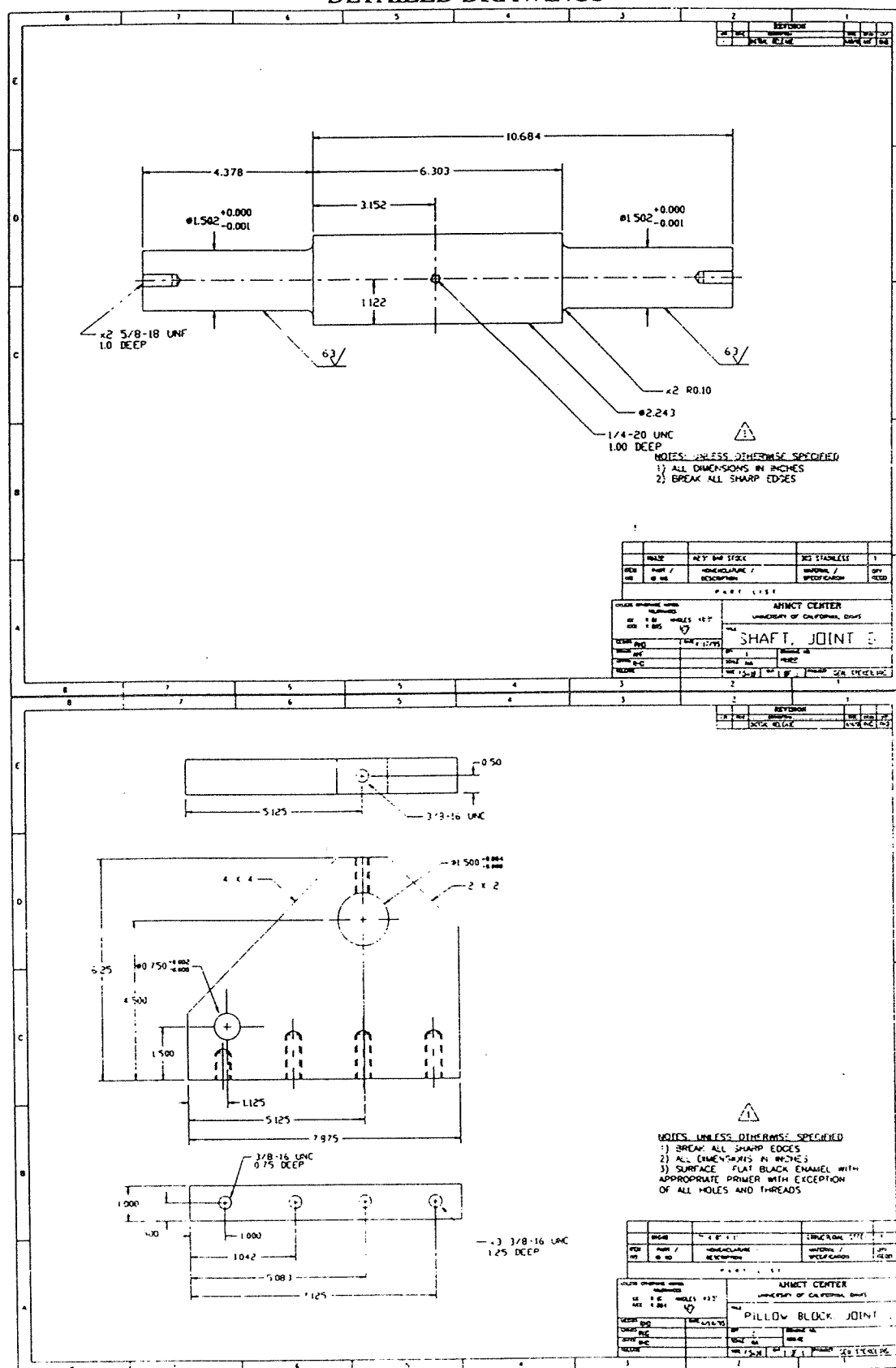NOTES: UNLESS OTHERWISE SPECIFIED
1) BREAK ALL SHARP EDGES
2) ALL DIMENSIONS IN INCHES
3) ANODIZE BLACK

X4 5/16-18 UNC

X8 ⌀0.328
CSK FOR 5/16-18 FLAT
HEAD SOCKET CAP SCREW

0.500

PLATE, JOINT F-1

M1086

0.500

SECTION A-A

CSK FOR 5/8-11
FLAT HEAD
SOCKET CAP SCREW

△1

NOTES: UNLESS OTHERWISE SPECIFIED
1) BREAK ALL SHARP EDGES
2) ALL DIMENSIONS IN INCHES
3) NEGLECT COUNTERSINK ON THESE
PARTS

JOINT WASHER

APPENDIX B
DETAILED DRAWINGS

0.400

A

Ø1.500

Ø0.50
CSK FOR 1/2-13
FLAT HEAD
SOCKET CAP SCREW

SECTION A-A   A

NOTES UNLESS OTHERWISE SPECIFIED
1) BREAK ALL SHARP EDGES
2) ALL DIMENSIONS IN INCHES

JOINT WASHER (CM)

104.500

NOTES UNLESS OTHERWISE SPECIFIED
1) ALL DIMENSIONS ARE IN INCHES
2) BREAK ALL SHARP EDGES
3) TUBES SHOULD BE WITHIN ... IN LENGTH OF EACH OTHER
4) FACE BOTH ENDS
5) ANODIZE TUBE AFTER MACHINING

LINK ABD/DEF TUBE
M1103

APPENDIX B
DETAILED DRAWINGS

NOTES: UNLESS OTHERWISE SPECIFIED
1) ALL DIMENSIONS ARE IN INCHES
2) BREAK ALL SHARP EDGES
3) FACE BOTH ENDS
4) ALODINE TUBE AFTER MACHINING

73.800

AHMCT CENTER

LINK TUBE

45° X .06
R0.01 MAX

NOTES: UNLESS OTHERWISE SPECIFIED
1) ALL DIMENSIONS IN INCHES
2) PART IS SYMMETRICAL ABOUT CENTER LINE

AHMCT CENTER

LINKAGE PIN

APPENDIX B
DETAILED DRAWINGS

Ø1.57 — Ø1.448

106.00

⚠

NOTES UNLESS OTHERWISE SPECIFIED
1) ALL DIMENSIONS IN INCHES

AHMCT CENTER
UNIVERSITY OF CALIFORNIA, DAVIS

LINKAGE TUBING
M11

8.993 ±0.001

Ø1.500 +0.000 -0.001
FOR LIGHT PRESS
FIT OF 1.500 DIA
CAM FOLLOWER
(PROVIDED)

Ø0.625 +0.000 -0.000

R0.82

BOTH SIDES TANGENT
TO THE TWO RADII

1.000

⚠

NOTES UNLESS OTHERWISE SPECIFIED
1) BREAK ALL SHARP EDGES
2) ALL DIMENSIONS IN INCHES
3) ANODIZE BLACK
4) PRESS THE PROVIDED CAM FOLLOWER
INTO THE Ø1.500 HOLE

AHMCT CENTER
UNIVERSITY OF CALIFORNIA, DAVIS

D-H LINKAGE
M133

APPENDIX B
DETAILED DRAWINGS

⌀0.626 ±0.001

⌀1.00

1.389

NOTES: UNLESS OTHERWISE SPECIFIED
1) BREAK ALL SHARP EDGES
2) ALL DIMENSIONS IN INCHES
3) ANODIZE BLACK

COLLAR, JOINT H
M1134

3.00

7/8-14 UNF
1.50 MIN THREAD DEPTH
DRILL THRU WITH TAP DRILL

NOTES: UNLESS OTHERWISE SPECIFIED
1) BREAK ALL SHARP EDGES
2) ALL DIMENSIONS IN INCHES

LINKAGE INSERT
M1135

APPENDIX B
DETAILED DRAWINGS

APPENDIX B
DETAILED DRAWINGS

⌀0.626 ±0.001

1.000

⌀1.00

NOTES: UNLESS OTHERWISE SPECIFIED
1) BREAK ALL SHARP EDGES
2) ALL DIMENSIONS IN INCHES

COLLAR, POINT

TAP HOLE 5/8-11 UNC THRU
AFTER PLATE AND BLOCK
ARE ASSEMBLED

NOTES: UNLESS OTHERWISE SPECIFIED
1) BREAK ALL SHARP EDGES
2) ALL DIMENSIONS IN INCHES

ASSEMBLY, JOINT

APPENDIX B
DETAILED DRAWINGS

APPENDIX B
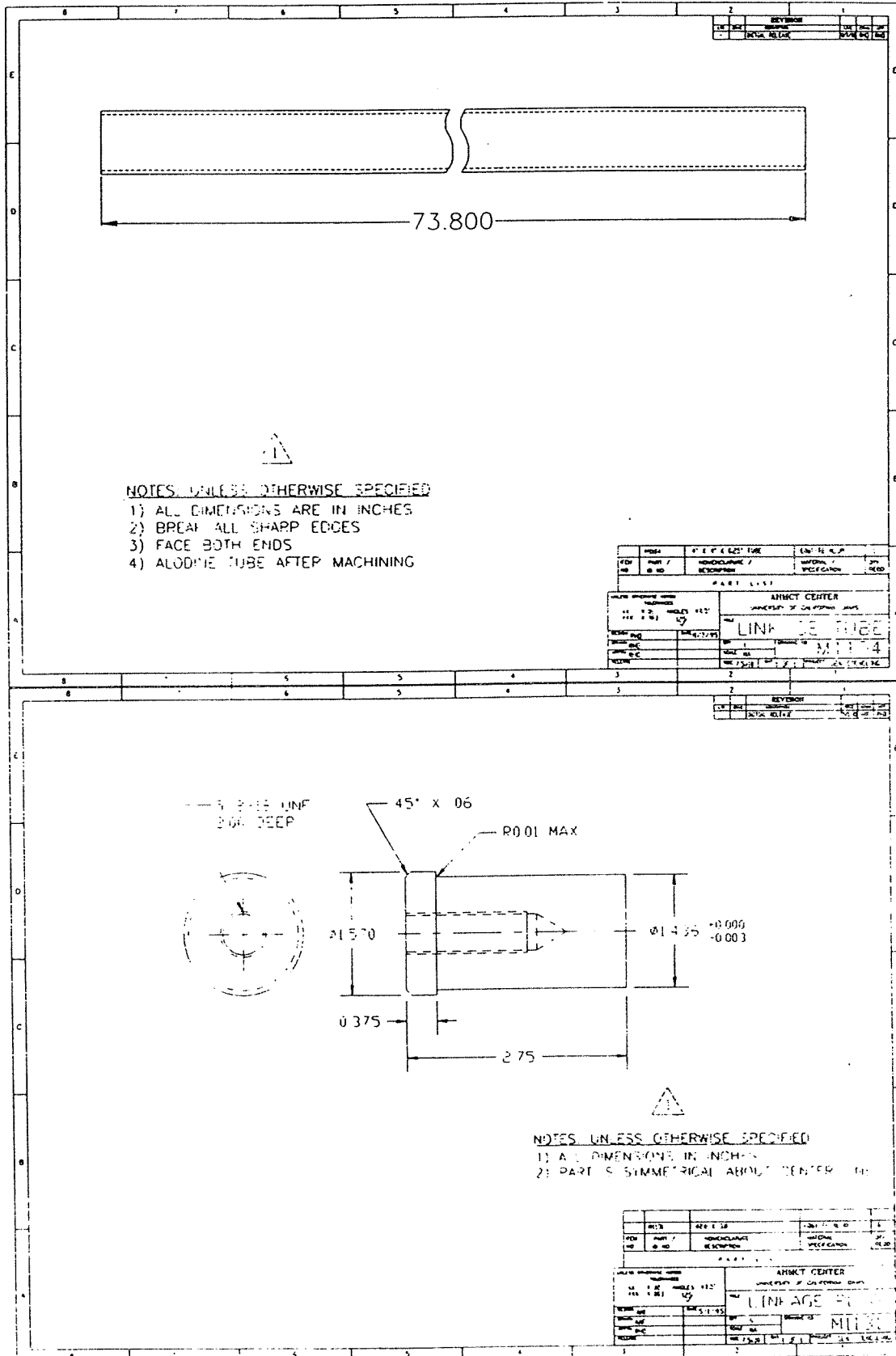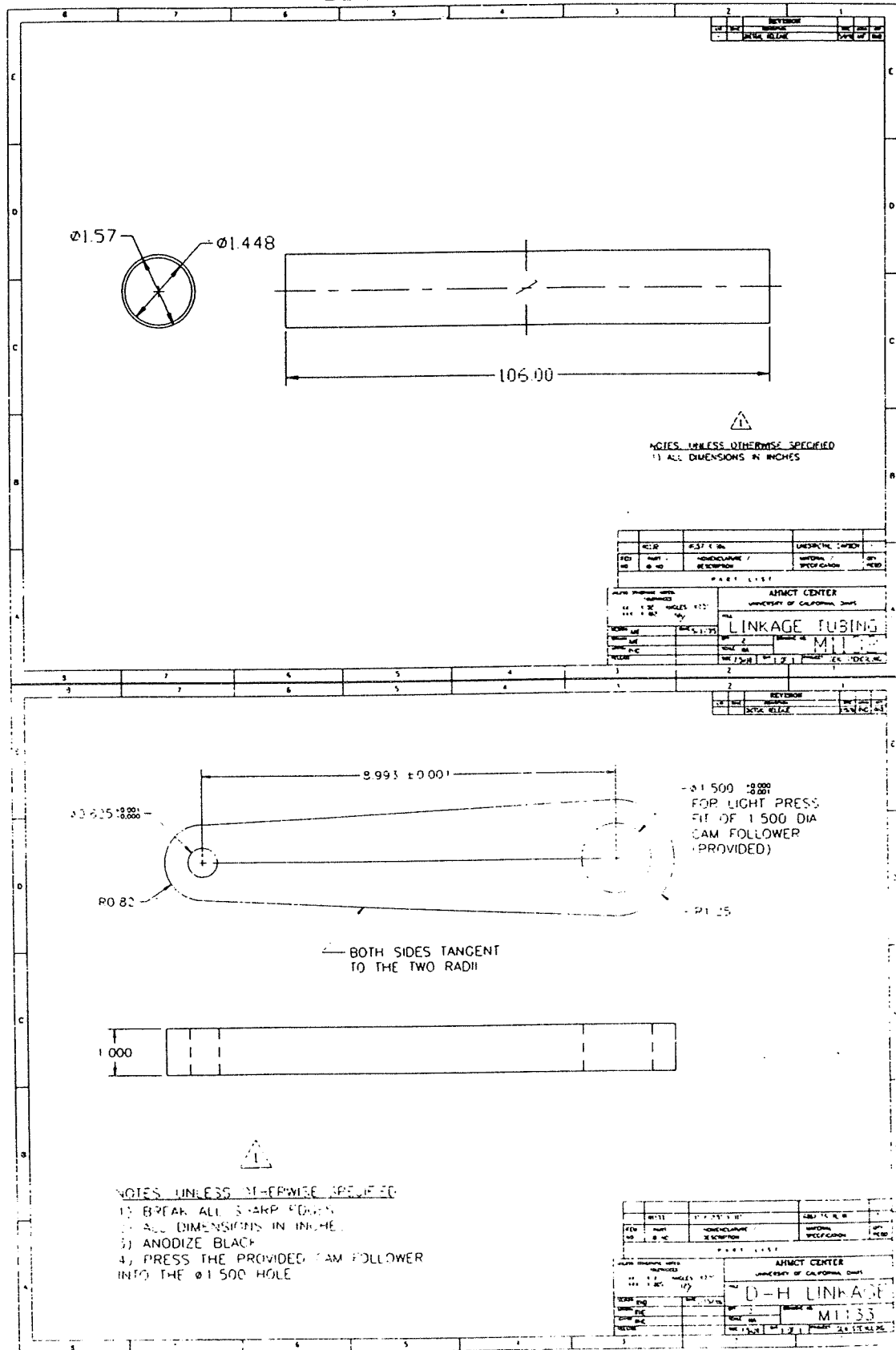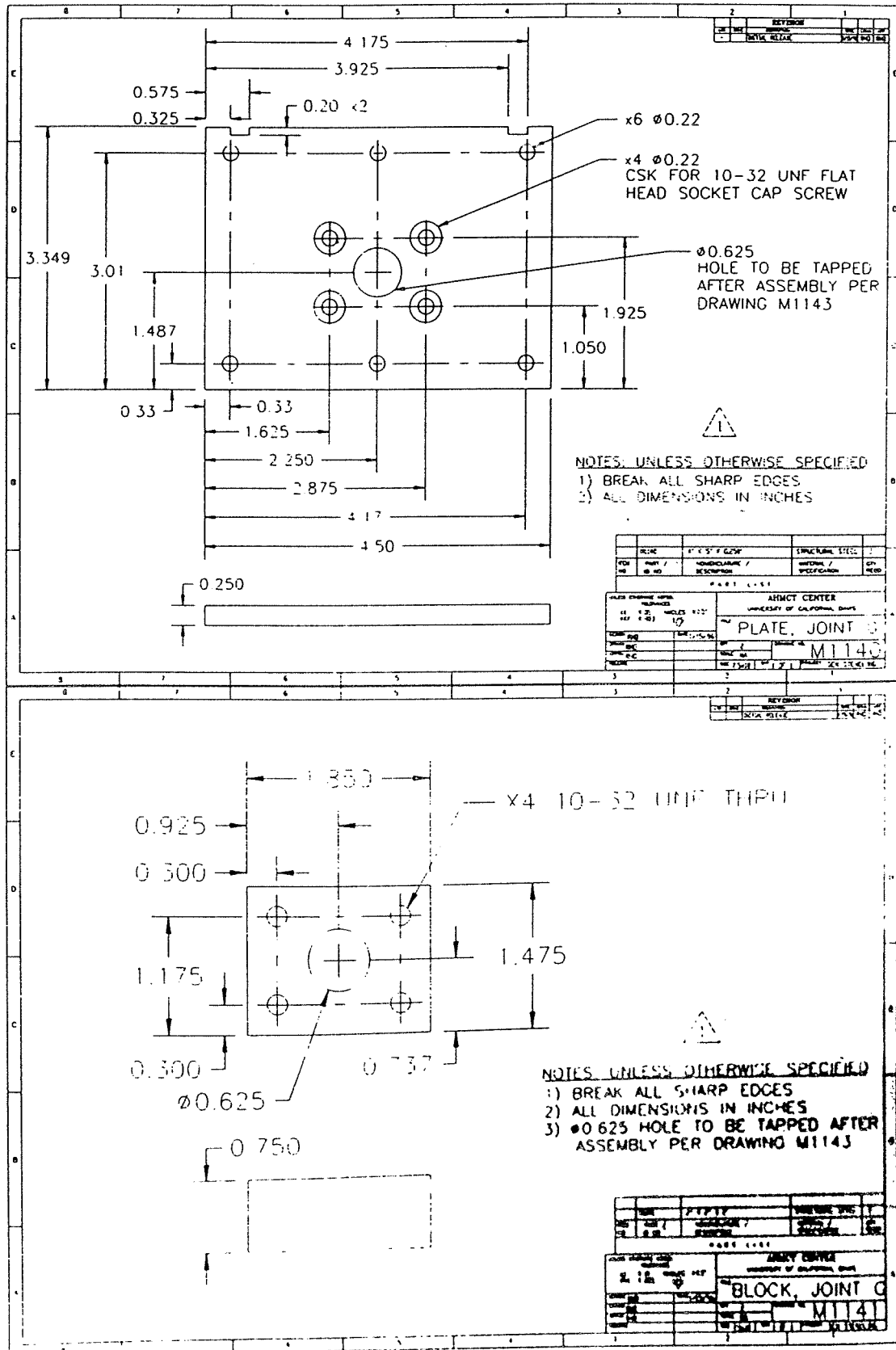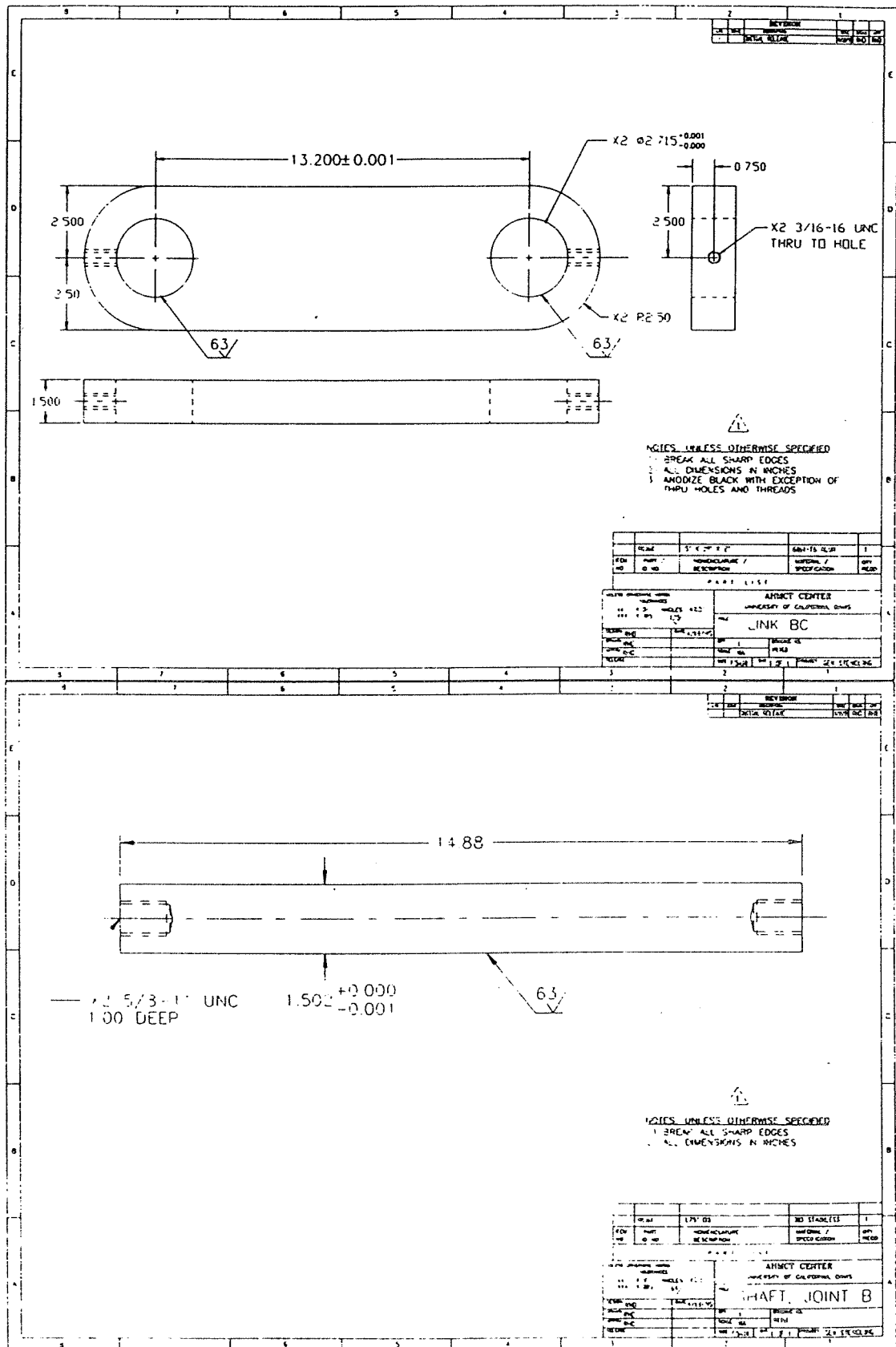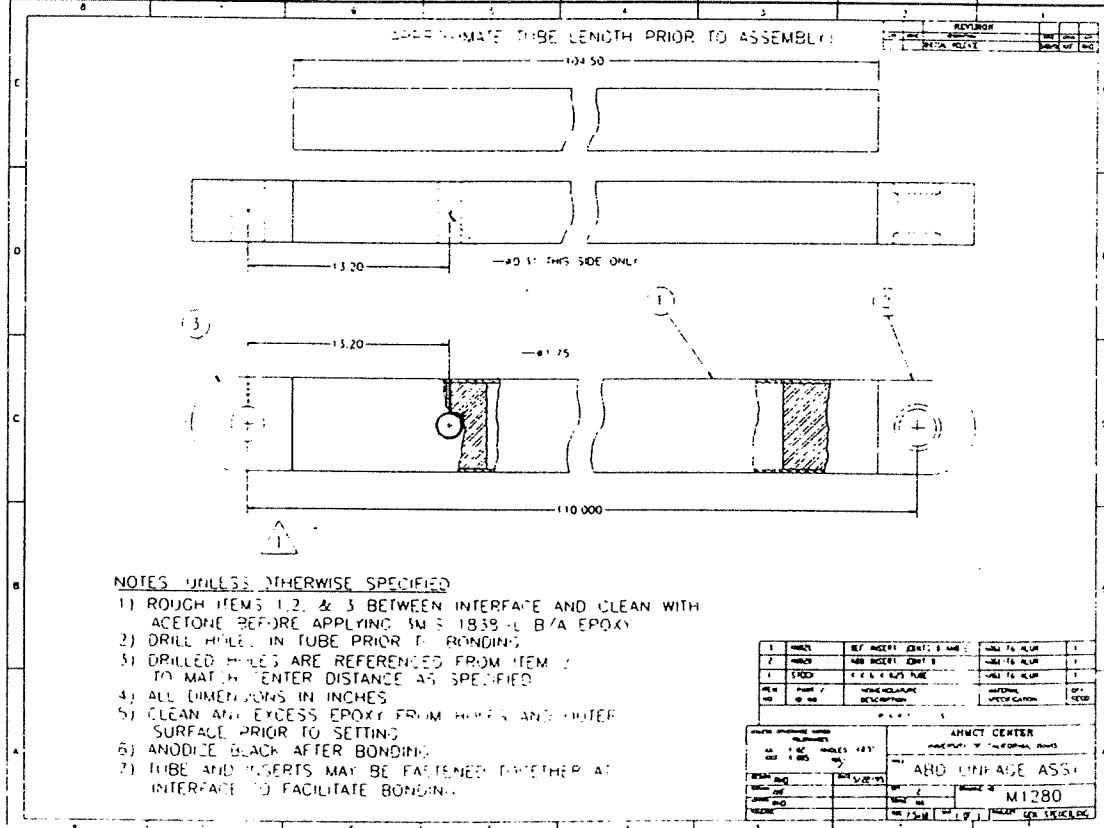## DETAILED DRAWINGS
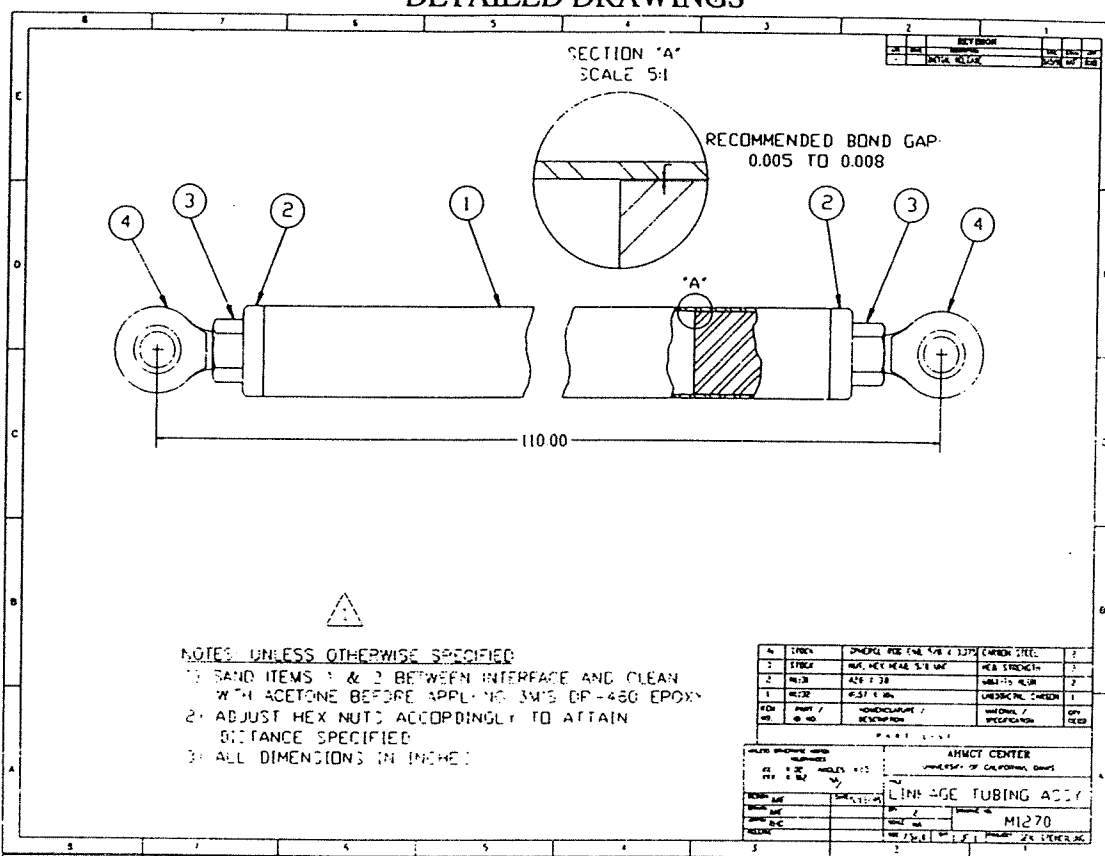
APPENDIX B
DETAILED DRAWINGS

SECTION 'A'
SCALE 5:1

RECOMMENDED BOND GAP
0.005 TO 0.008

'A'

— 110.00 —

NOTES UNLESS OTHERWISE SPECIFIED
1) SAND ITEMS 1 & 2 BETWEEN INTERFACE AND CLEAN
   WITH ACETONE BEFORE APPLYING 3M'S DP-460 EPOXY
2) ADJUST HEX NUTS ACCORDINGLY TO ATTAIN
   DISTANCE SPECIFIED
3) ALL DIMENSIONS IN INCHES

AHMCT CENTER
UNIVERSITY OF CALIFORNIA, DAVIS
LINKAGE TUBING ASSY
M1270

APPROXIMATE TUBE LENGTH PRIOR TO ASSEMBLY

— 104.50 —
— 15.20 —
— 15.20 —

— 110.000 —

NOTES UNLESS OTHERWISE SPECIFIED
1) ROUGH ITEMS 1,2, & 3 BETWEEN INTERFACE AND CLEAN WITH
   ACETONE BEFORE APPLYING 3M'S 1838-L B/A EPOXY
2) DRILL HOLES IN TUBE PRIOR TO BONDING
3) DRILLED HOLES ARE REFERENCED FROM ITEM 2
   TO MATCH CENTER DISTANCE AS SPECIFIED
4) ALL DIMENSIONS IN INCHES
5) CLEAN ANY EXCESS EPOXY FROM HOLES AND OUTER
   SURFACE PRIOR TO SETTING
6) ANODIZE BLACK AFTER BONDING
7) TUBE AND INSERTS MAY BE FASTENED TOGETHER AT
   INTERFACE TO FACILITATE BONDING

AHMCT CENTER
UNIVERSITY OF CALIFORNIA, DAVIS
ABD LINKAGE ASSY
M1280

APPENDIX B
DETAILED DRAWINGS